PEPTIDE HYDROGELS CONTAINING CELL ATTACHMENT MOLECULES

A Thesis Submitted to
the Graduate School of Engineering and Science of
İzmir Institute of Technology
in Partial Fulfillment of the Requirements for the Degree of

MASTER OF SCIENCE

in Chemical Engineering

by
Berk UYSAL

July 2019
İZMİR

We approve the thesis of **Berk UYSAL**

Examining Committee Members:

Assist. Prof. Dr. Ayben TOP

Department of Chemical Engineering, İzmir Institute of Technology

Prof. Dr. Muhsin ÇİFTÇİOĞLU

Department of Chemical Engineering, İzmir Institute of Technology

Assist. Prof. Dr. Çisem BULUT ALBAYRAK

Department of Food Engineering, Adnan Menderes University

19 July 2019

Assist. Prof. Dr. Ayben TOP

Supervisor, Department of Chemical Engineering, İzmir Institute of Technology

Prof. Dr. Erol ŞEKER

Head of the Department of Chemical Engineering

Prof. Dr. Aysun SOFUOĞLU

Dean of the Graduate School of Engineering and Sciences

ACKNOWLEDGMENTS

I would like to express my gratitude for my advisor Assist. Prof. Dr. Ayben TOP for her helps throughout this study. It would not have come to fruition without her invaluable presence, experience, supervision and concern. It has been a privilege to work with her.

I would also like to express my gratitude to my committee members, Prof. Dr. Muhsin ÇİFTÇİOĞLU and Assist. Prof. Dr. Çisem BULUT ALBAYRAK for their suggestions and recommendations. I would like to thank Prof. Dr. Muhsin ÇİFTÇİOĞLU yet again for making rheological experiments possible.

Prof. Dr. Talat YALÇIN was greatly indebted to for performing MALDI-TOF mass spectroscopy experiments at Biological Mass Spectrometry and Proteomics Facility located at the Chemistry Department. I appreciate the help I received from Filiz KURUCAOVALI from Environmental Development Application and Research Center, and, Özlem ÇAĞLAR DUVARCI and Deniz ŞİMŞEK from Department of Chemical Engineering during the characterization studies.

I am especially grateful for the companies I had during my studies, Berk TÜRKKUL, Bertan ÖZDOĞRU, Emre DEĞİRMENCİ, Damla YALÇIN, Merve DİKMEN, Özgün DELİİSMAİL, Elif GÜNGÖRMÜŞ DELİİSMAİL, Pınar ÇETİN, Selin ÖZKIYICI, and many more that I may or may not have missed.

Last, but not least, I am immensely grateful for the support I received by my family throughout not just this part, but my whole life. Without them, none of this would have ever happened.

ABSTRACT

PEPTIDE HYDROGELS CONTAINING CELL ATTACHMENT MOLECULES

In this study, peptides with sequences and notations as KLELKLELKLEL (KLEL), KLDVKLDVKLDV (KLDV), KLDVKLDVKLKV (KLKV1), KLKVKLDVKLKV (KLKV2), KLKVKLKVKLKV (KLKV3) were synthesized using solid phase peptide synthesis (SPPS) method based on Fmoc chemistry. Reverse phase HPLC and MALDI-TOF mass spectroscopy characterization methods were used to assess the purity of the peptides. Three different synthesis procedures were tested, and it was found that employing DMF:DMSO at 1:1 ratio as a solvent increased purity of the resultant peptide. FTIR results indicated the presence of expected β-sheet secondary structure, as well as an interference band from TFA salts for all of the peptides. All the peptides formed hydrogels at pH 7.4 with 1 wt% concentration in deionized water (DIW). AFM results of these hydrogels indicated that KLKV1 and KLKV2 had fibrous morphology with a width of 5-20 nm and 7-18 nm respectively. KLDV and KLKV3 peptide hydrogels, on the other hand, exhibited globular structures, having sizes with 15-50 nm and 8-15 nm, respectively. Storage moduli (G') of these hydrogels in DIW were obtained as ~860 ± 150 Pa, ~260 ± 60 Pa, ~210 ± 30 Pa and ~1850 ± 200 Pa for KLDV, KLKV1, KLKV2 and KLKV3 respectively. Of these peptides, only HCl salt of KLDV and KLKV1 peptides more readily formed hydrogels in PBS but at 1.5 wt% concentration. G' values of these KLDV and KLKV1 hydrogels were determined as ~1810 ± 850 Pa and ~700 ± 230 Pa, respectively. Cell proliferation tests (CCK-8 assay) of KLDV and KLKV1 hydrogels were performed by using L929 mouse fibroblast cells. Empty wells (TCPS) were used as a control group. Cell proliferation was observed to be comparable for both select hydrogels and empty wells, suggesting possible applications of these hydrogels in tissue engineering.

ÖZET

HÜCRE YAPIŞMA MOLEKÜLLERİ İÇEREN PEPTİD HİDROJELLER

Bu çalışmada KLELKLELKLEL (KLEL), KLDVKLDVKLDV (KLDV), KLDVKLDVKLKV (KLKV1), KLKVKLDVKLKV (KLKV2), KLKVKLKVKLKV (KLKV3) dizinleri ve kısaltmalarına sahip peptidler, f-moc kimyası temelli katı faz peptid sentez yöntemi (SPPS) kullanılarak sentezlenmiştir. Peptidlerin saflığını değerlendirmek için ters faz HPLC ve MALDI-TOF kütle spektroskopisi karakterizasyon yöntemleri kullanılmıştır. 3 farklı sentez prosedürü test edilmiştir ve çözgen olarak 1:1 oranda DMF:DMSO kullanılmasının, elde edilen peptidin saflığını artırdığı bulunmuştur. FTIR sonuçları, tüm peptidler için beklenen β-sheet ikincil yapısıyla birlikte, TFA tuzlarından gelen girişim bandını göstermiştir. Bütün peptidler, ağırlıkça 1% derişim, pH 7.4 ve deiyonize su içerisinde hidrojel oluşturmuştur. Bu hidrojellerin AFM sonuçları, KLKV1 ve KLKV2'nin, sırasıyla 5-20 nm ve 7-18 nm genişlikte lifli morfolojiye sahip olduğunu göstermiştir. Diğer taraftan, KLDV ve KLKV3 peptid hidrojelleri, sırasıyla, 15-50 nm ve 8-15 nm boyutları arasında küresel yapılar sergilemiştir. Deiyonize suda hazırlanan bu hidrojellerin, saklama modülleri, KLDV, KLKV1, KLKV2 ve KLKV3 için, sırasıyla, ~860 ± 150 Pa, ~260 ± 60 Pa, ~210 ± 30 Pa ve ~1850 ± 200 Pa olarak elde edilmiştir. Bu peptidlerden, sadece KLDV ve KLKV1 peptidlerinin HCl tuzları, PBS içerisinde, ağırlıkça 1.5% derişimde hidrojel oluşturmuştur. Bu KLDV ve KLKV1 hidrojellerinin G' değerleri, sırasıyla ~1810 ± 850 Pa ve ~700 ± 230 Pa olarak belirlenmiştir. KLDV ve KLKV1 hidrojellerinin hücre çoğalma testleri (CCK-8 analizi) L929 fare fibroblast hücreleri kullanılarak yapılmıştır. Boş kuyucuklar (TCPS) control grubu olarak kullanılmıştır. Her iki seçilmiş hidrojel ve boş kuyucuklar için hücre çoğalması karşılaştırabilir olarak gözlenmiş ve sonuç olarak bu hidrojellerin doku mühendisliğinde muhtemel uygulamaları olabileceğini önermektedir.

TABLE OF CONTENTS

LIST OF FIGURES

Figure **Page**

Figure **Page**

LIST OF TABLES

Table **Page**

CHAPTER 1

INTRODUCTION

Hydrogels are of three-dimensional matrices that are hydrophilic and capable of retaining a significant amount of water or biological fluid when swollen. Due to their porous structure, swelling ability and viscoelastic properties they can simulate natural living tissue very closely. Additionally, their various tunable properties make hydrogels an excellent choice of synthetic biomaterials. (Schnepp et al. 2006, Jayawarna et al. 2006, Mahler et al. 2006). Not surprisingly, hydrogels have been used for biomedical purposes for decades, due to their structure closely mimicking extracellular matrix (ECM), thus making it an excellent choice for cell growth landscape. Various uses of hydrogels included but not limited to cell encapsulation, wound healing, injury recovery, as well as for delivering drugs, antibodies, proteins, nucleic acids and growth factors (Lee and Mooney 2001).

Hydrogels can be grouped under various categories, depending on the material source, ionic charge, preparation method, physical properties, crosslinking, degradability and response. Physical hydrogels have gained significance due to the lack of any crosslinking agents which may possess harmful properties, as well as the relative ease of the preparation process (Zhang et al. 2004). Polymers, both natural and synthetic, polypeptides, and peptides were reported to form physical hydrogels upon judicious choice of their structures, compositions, and molecular weight.

Peptide-based hydrogels are oligomers of naturally occurring amino acids, therefore they are biodegradable, biocompatible and generally non-immunogenic. They are precisely controlled and chemically defined, not requiring complex work-up by offering much safer bio-applications (Jonker et al. 2012). Additionally, particular peptide sequences may act as biological cues. For example, arginine-glycine-aspartic acid (RGD) containing hydrogels are able to improve cell attachment. Another integrin binding motif, leucine-aspartic acid-valine (LDV) was also shown to mediate cell-binding events. Different from RGD sequence, LDV can participate alternating hydrophobic-hydrophilic repeats, a common β-sheet forming motif observed in most of the peptide hydrogels. The aim of this study is to synthesize a physical hydrogel capable of self-assembly at

physiologic conditions, which inherently contains the cell attachment unit composed of LDV sequence, thus promoting cell activity without requiring any other adduct.

In the following section (Chapter 2), more extensive information on hydrogels was given, followed by the studies on the effect of crosslinking on hydrogels, the effect of biological cues on bio-applications of hydrogels, as well as design and applications of peptide hydrogels.

Chapter 3 contains the materials used in the experiments and the experimental details including synthesis methods of the peptides with their primary characterization and preparation and characterization of the peptide-based hydrogels.

In Chapter 4, purity assessments of the peptides synthesized via different methods along with the results of the conformation of the peptides are given. Additionally, the results of the characterization of the prepared hydrogels, such as the morphology and rheology as well as the cell proliferation results were discussed.

Chapter 5 concludes the thesis study and outlines a proposal for a continuation of new experiments, which includes next level characterization studies.

CHAPTER 2

LITERATURE SURVEY

This chapter represents a brief literature study about hydrogels, their classifications, with a special emphasis on peptide-based hydrogels; their design, applications and hydrogels, which contain biological cues.

2.1. Hydrogels

Hydrogels are three-dimensionally structured hydrophilic polymer networks that are capable of absorbing and preserving high amounts of water and/or biological fluids. Basic elements of a hydrogel are given in Figure 2.1. They can be produced based on wide variety of natural and synthetic materials, including but not limited to carbohydrates, natural gums, polyacrylates, silicone, collagen, gelatin, alginate, proteins and peptides. Their tunable properties, biodegradability, biocompatibility and their ability to mimic living tissue due to the structural similarities of hydrogels and extracellular matrices (ECM) highlights them as a remarkable sub-group of biomaterials (Schnepp et al. 2006, Jayawarna et al. 2006, Mahler et al. 2006).

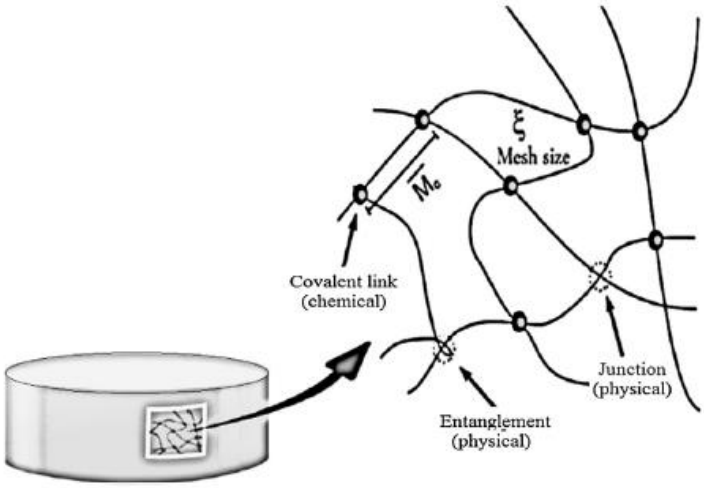

Figure 2.1. Basic elements of a hydrogel (Source: Ullah et al. 2015)

Problems such as the insolubility, high crystallinity, lack of biodegradability, unfavored properties for both mechanical and thermal conditions and the toxicity of crosslinkers have been some of the main limitations of the hydrogels, thus, requiring further development in this area. Crosslinking preserves the integrity of the hydrogels during swelling, which can take place in vitro, during preparation, or in-vivo, after insertion into physiological conditions. Additionally, crosslinking points can counterbalance the solubility by retractive forces, thus maintaining the equilibrium of the swelling (Ullah et al. 2015). Without any crosslinking, on the other hand, the hydrophilic polymer chains would dissolve within water.

Hydrophilic property of a crosslinked network is due to the hydrophilic sidechains such as $-NH_2$, -COOH, -OH, $-CONH_2$, -CONH- and $-SO_3H$. Hydrophilic properties, coupled with the crosslinking points, is the reason why the 3-D structure of the hydrogels is maintained in a swollen state.

Hydrogels can be classified under several subgroups, depending on the source, ionic charge, preparation method, physical properties, crosslinking, degradability and response as given in Figure 2.2.

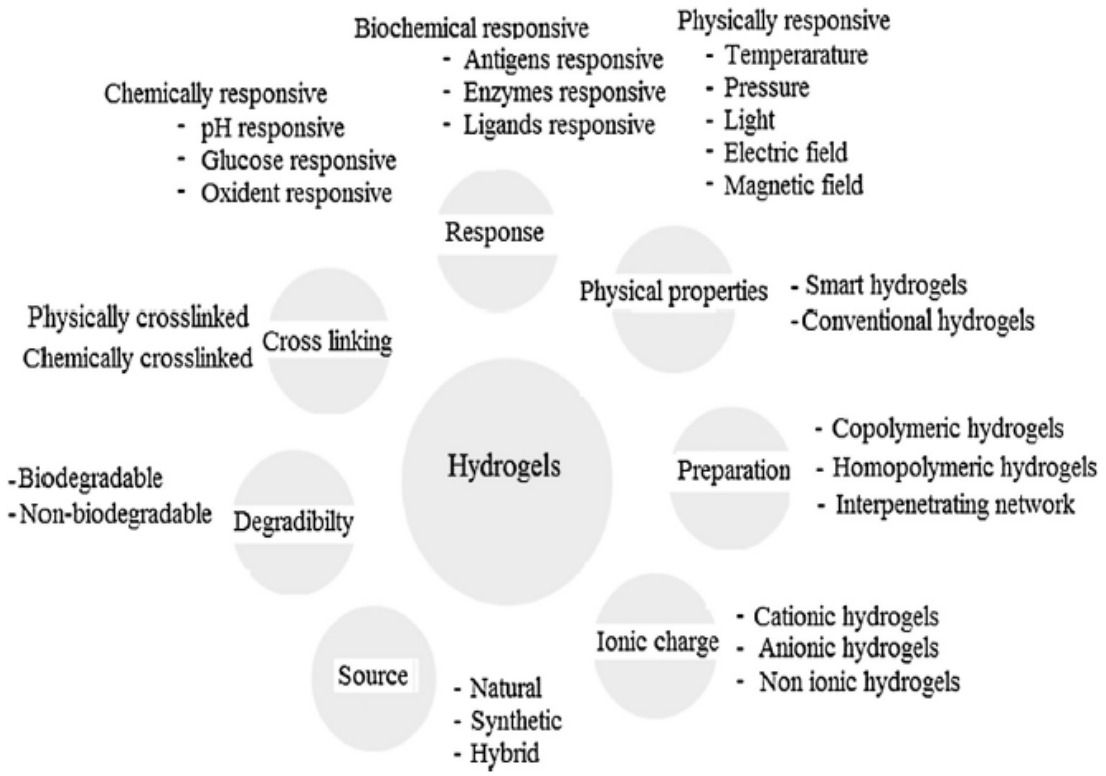

Figure 2.2. Classification of hydrogels (Source: Ullah et al. 2015)

Although there are various classifications of hydrogels, they can also be divided into two main categories as physical and chemical hydrogels, due to the fact that hydrogels are basically constructed by crosslinked networks. Basic preparation routes of physical and chemical hydrogels are given in Figure 2.3.

Physical hydrogels (also referred to as reversible or self-assembled hydrogels) have gained significance due to their ease of production in comparison with chemical hydrogels, as well as the lack of crosslinking agent by offering more cytocompatibility. They are formed through physical interactions between different chains, such as van der Waals forces, hydrogen bonding and hydrophobic interactions.

Chemical hydrogels are formed via covalent bonding, thus, forming a much sturdier gel as a final structure, lacking the flexibility of physical hydrogels, yet possessing a stronger and more stable structures that are near impossible to dissolve unless crosslinking points are cleaved.

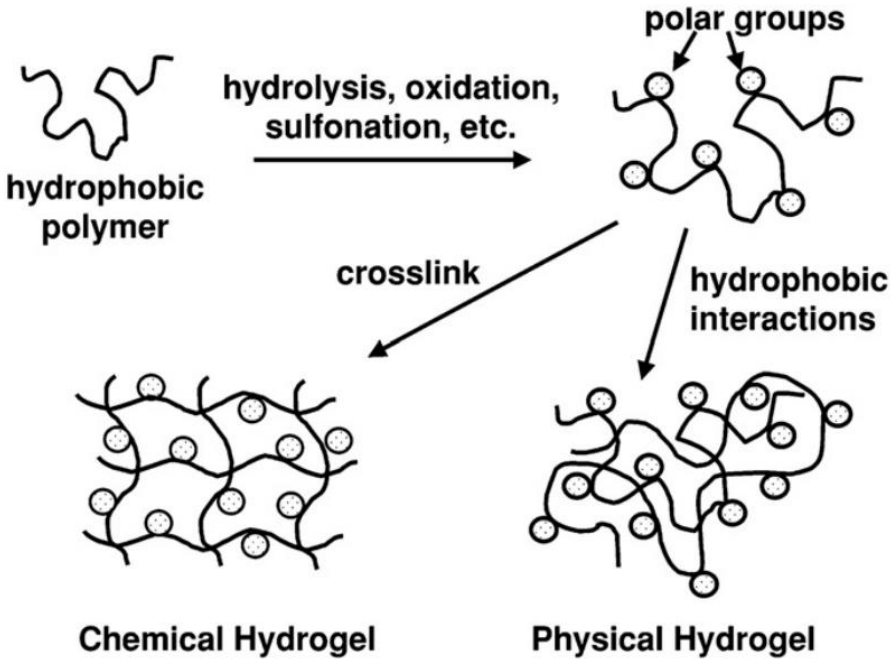

Figure 2.3. Basic preparation routes of physical and chemical hydrogels (Source: Chirani et al. 2015)

Hydrogels are used extensively in the biomedical field including tissue engineering, drug, protein and gene delivery, along with bio-sealants, wound healing, injury recovery, bio-adhesives and cell encapsulation applications (Chung and Park 2009).

2.2. Physical Hydrogels

Physical hydrogels, also referred to as self-assembled hydrogels, are hydrogels crosslinked by physical interactions, as given in Figure 2.4. which also renders them reversible. They have gained significant attention due to their ease of production, as well as the lack of toxicity that may stem from the nature of chemical crosslinking agents. Physical crosslinking can occur via hydrogen bonding, stereocomplex formations, ionic interactions and protein interactions and can be tuned by temperature, pH, processing methods, and composition of the gel forming materials as outlined in the following studies.

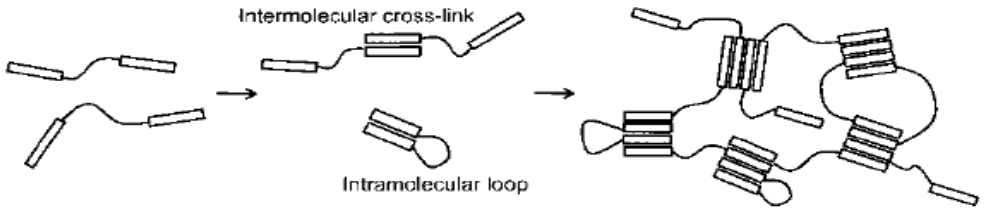

Figure 2.4. Physically crosslinked Hydrogels (Source: Dooling and Tirrell 2013)

Yokoyama et al. (1986) studied poly(vinyl alcohol) (PVA) hydrogels. It was known that PVA hydrogels form gradually at room temperature, but possessing quite low mechanical strength. It was then found out that repeated freeze-thawing process turned PVA hydrogels into sturdier and highly elastic gels instead, without any additions. The end results were largely dependent on the concentration of PVA in water, molecular weight of PVA, freezing time and temperature, as well as the number of freeze-thawing cycles.

Alginates are well-known examples of polymers that can be crosslinked by ionic interactions with calcium ions. Alginate crosslinking can be carried out at physiological pH and room temperature, and the nature of alginate can easily alter the pore size, degradation rate and release kinetics, therefore making it suitable as a matrix to encapsulate living cells, as well as proteins (Goosen et al. 1985, Gombotz and Wee 1998, Gacesa 1988).

Tirrell and Cappello pioneered into a new field in chemistry, called protein engineering. The major advantage of proteins is that their physical and chemical properties can be modified and tuned as desired by changing the protein sequence

composed of naturally occurring amino acids and/or synthetic ones. Cappello and his coworkers synthesized sequential block copolymers containing silk-like and elastin-like block repeats, in which the insoluble silk-like segments are associated via hydrogen bonded β-sheet or strand forms, called 'prolastins'. These block copolymers are soluble in water, but they can undergo irreversible sol-gel transition under physiological conditions due to the crystallization of silk-like domains, and can also be easily mixed with drugs. The release and gelation rates were reported to be dependent on various parameters, such as concentration, temperature and composition (Cappello et al. 1990, Cappello et al. 1998).

2.3. Chemical Hydrogels

Chemically crosslinking of the hydrogels, though they may have toxic effects, have been preferred in many applications for providing a much sturdier, stronger, and long-lasting hydrogel. Unlike the preparation of physical hydrogels, chemical crosslinking process is irreversible due to the formation of a covalent bond as given in Figure 2.5. Chemical crosslinking can be mediated by various types of reactions such as addition reactions, complementary chemical reactions, irradiation and enzymatic reactions. Following studies will be providing a deeper insight into the various forms of chemical crosslinking.

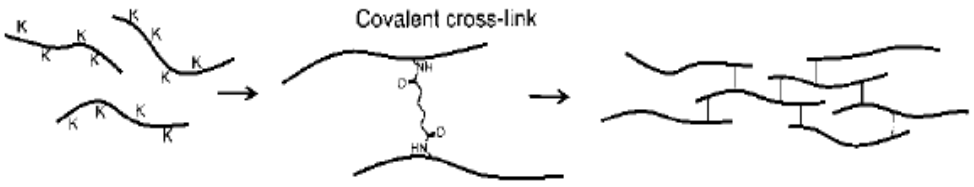

Figure 2.5. Schematic representation of the assembly of a chemically crosslinked hydrogel (Source: Dooling and Tirrell 2013)

Reaction of crosslinking agents having two or more functional groups with-soluble polymers is one of the strategies to form hydrogels. Polysaccharides with complementary functional groups were shown to be crosslinked via 1,6-hexamethylenediisocyanate (Brondsted et al. 1995), divinylsulfone (Gehrke et al. 1998),

or 1,6-hexanedibromide (Coviello et al. 1999).

High energy radiation, mainly gamma and electron beams, which can be used to polymerize unsaturated compounds, can promote gelation of water-soluble polymers with vinyl groups. Mohd Amin et al. (2012) prepared hydrogels using bacterial cellulose (BC), a natural polymer, grafted with acrylic acid (AA). Both thermo and pH responsive hydrogel were obtained by exposing grafted polymer to accelerated electron-beam radiation at varying doses. Alla et al. (2012) obtained hydrogels based on tara gum/acrylic acid (TG/AA), by using gamma irradiation and N,N-methylenebisacrylamide (MBAAm) as a crosslinking agent.

Water-soluble polymers with hydroxyl groups can be crosslinked via glutaraldehyde. However, the requirements for the crosslinking reactions are drastic, such as low pH, and high temperature, limiting its applications. Amine containing polymers, on the other hand, can be crosslinked under mild conditions with glutaraldehyde, forming Schiff bases, as used for gelatin (Yamamoto et al. 2000), albumin (Willmott et al. 1984) and amine containing polysaccharides (Jameela and Jayakrishnan 1995). The toxicity of the glutaraldehyde even at low concentrations could cause cell growth inhibition. For this reason, more cytocompatible crosslinking agents such as polyaldehydes obtained by the partial oxidation of dextran have been usually preferred.

Free radical polymerization of polymerizable group of derivatized hydrophilic polymers can also yield chemically crosslinked hydrogels, Patil and his coworkers introduced methacrylic groups to sucrose by using optimase M440 enzyme as a catalyst to prepare sucrose acrylate monomer, which, then, was polymerized and crosslinked with methylene bisacrylamide (BIS) at different ratios to form hydrogels. (Patil et al. 1996, Patil et al. 1997). Hubbell et al. (1996) showed that photopolymerization can also be used to promote gelation of acrylate form of a poly(lactic acid) (A) poly(ethylene glycol) (B) ABA block copolymer by using a photoinitiation and cocatalyst system (Hubbell 1996).

In another study, Sperinde and Griffith (1997) prepared enzymatically crosslinked PEG hydrogel. First, tetrahydroxy PEG (PEG-(OH)4) was functionalized by with glutaminyl (Q) groups to form PEG-Q_a. Then, formation of PEG-polypeptide network was observed after the addition of trans-glutaminase into the aqueous solution of PEG-Q_a and poly(lysine-co-phenylalanine). Gelation was due to the amide bond formation as a result of the transglutaminase catalyzed reaction between the γ-carboxamide groups of the PEG-Q_a and the ε-amine group of lysines of the polypeptide.

2.4. Hydrogels Containing Biological Cues

Integrins are a family of cell adhesion receptors, one of the major ones, which are non-covalently linked, heterodimeric molecules that contain α and β subunits. These subunits are type I transmembrane proteins that contain large extracellular domains and mostly short cytoplasmic domains. Cytoplasmic face coordinates the assembly of cytoskeletal polymers and signaling complexes whereas extracellular face engages with either ECM macromolecules or counter receptors on adjacent cell surfaces. There are 24 different α-β combinations that have been identified to date at the protein level, with 12 integrins containing the β1 subunit and five containing αV. Most integrin receptors can bind a wide variety of ligands as well as many ECM cell surface adhesion proteins can also bind multiple integrin receptors (Humphries et al. 2006). Fibronectin is one of the glycoproteins, involved in various biological processes, mainly in mediating cell attachment and migration. Further studies on fibronectin has revealed some of the short peptide sequences that are identified as adhesion recognition sequences, including Arg-Gly-Asp (RGD) and Leu-Asp-Val (LDV). RGD is recognized by all five αV, as well as two β1 integrins. However, LDV is recognized by a more limited subset of integrins, four from the β2 subfamily instead yet the functionality is still similar to RGD. Inclusion of RGD or LDV motifs on a synthetic peptide sequence was observed to provide ability to mimic the activity of intact proteins, at least partially as demonstrated in many studies (Yamada 1991).

Yang et al. (2005) incorporated Arg-Gly-Asp (RGD) sequence into poly (ethylene glycol) diacrylate (PEODA/PEGDA) polymers covalently in varying amounts. They showed that addition of RGD were resulted in 1344% increase in alkaline phosphatase (ALP) production and 277% increase in osteocalcin (OCN) accumulation, compared to the hydrogels lack of RGD sequences (Yang et al. 2005).

Shu et al. (2014a) studied the effect of the addition of RGD peptide sequence onto hyaluronan (HA) hydrogels, which are known to provide poor attachment and spreading of fibroblast and most mammalian cell types. They prepared the hydrogels by simply mixing a thiol-modified HA (3,3'-dithiobis(propanoic dihydrazide)) (HA-DTPH) and RGD containing PEG diacrylate (PEGDA) Upon the introduction of RGD groups, the attachment, spreading and proliferation of human and murine fibroblasts were significantly enhanced on the surface of the hydrogels . However, proliferation of the

encapsulated cells within the RGD containing hydrogels increased modestly compared to the control hydrogel lack of RGD sequence.

Veiga et al. (2012) proposed arginine-rich self-assembling peptide hydrogels possessing inherent antibacterial properties for wound healing application to prevent infection or kill an existing one. They simply modified lysine-rich, β-hairpin self-assembling peptide with a number of arginines ranging from 2 to 8 due to the fact that natural antimicrobial peptides (AMPs) have high arginine-residue content. The optimal value of number of arginines were found as 6, as further increase caused loss in the rigidity of the hydrogels with negligible increase in antibacterial activity. This optimal peptide hydrogel was shown to be potent antibacterial material against both gram-positive and gram-negative bacteria exhibiting cytocompatible and minimally hemolytic properties in mesenchymal stem cell culture.

Kang et al. (2014) prepared a number of self-assembling multidomain peptide (MPD) sequences containing cell attachment unit (RGDS) amd MMP-2 degradable sequence (SLRG) to observe the effect of sequence on morphology and expansion of encapsulated Stem cells from Human Exfoliated Deciduous teeth (SHED). They confirmed that RGDS motif accelerated initial cell attachment and spreading. More specifically, they also showed that the use of threonine instead of serine in the amphiphilic region required RGDS unit for the cell attachment whereas serine based MDPs were less selective and supported and increase in cell propagation regardless of the presence of RGDs.

Zhang et al. (2009) mixed two peptides, RGDA16 (Ac-RADARGDARADARGDA-CONH^2) and RADA16 (Ac-RADARADARADARADA-$CONH_2$), to observe the effects of the added RGD sequence on the attachment, spreading and proliferation of pre-osteoblasts (MC3T3-E1). It was shown that self-assembling peptide scaffold based on RADA-16 was already suitable to support cell attachment, survival and proliferation. As RGDA16 was unable to form hydrogel on its own, a mixture of RADA16 and RGDA16 at a 1:1 ratio, denoted as RGDAmix. was used to prepare hydrogel. They demonstrated that RGDAmix did provide significantly higher degree of cell attachment and proliferation for prolonged intervals, as expected.

Green and his coworkers integrated RGD sequence into the amphiphilic and anionic β-sheet forming peptide Pro-Asp-(Phe-Asp)$_5$-Pro, denoted as FD, which could assemble into a hydrogel that promoted the formation of bone mineral hydroxyapatite by the absorption of calcium and phosphate ions., They showed that the use of FD-RGD

hydrogel containing 25 mol% RGD increased the cell density almost two-fold compared to the sole FD hydrogel (Green et al. 2018).

2.5. Peptide Hydrogels

The development of peptide hydrogels requires a cross-disciplinary effort, by combining the structure and function data from biology and the synthesis and characterization methods provided by macromolecular chemistry and materials science fields. The main driving force behind the design of the novel peptide hydrogels can be described as the need for implantable scaffolds, benign methods for encapsulation, matrices for *in vitro* cell cultures and injectable delivery vehicles. Additionally, peptides can be designed to have the ability to undergo biochemical and structural changes depending on their response to pH and temperature changes, ligand binding, light and mechanical forces, which also suggests potential applications of peptide hydrogels as stimulus-responsive materials and in biosensors.

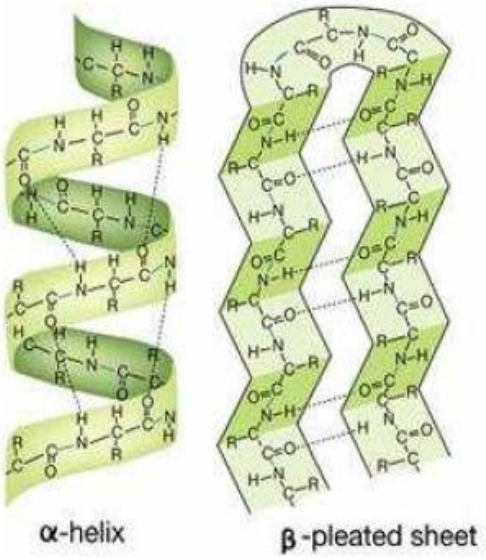

Figure 2.6. Representation of α-helix and β-sheet secondary structures (Source: Rashid et al. 2015)

Polymers formed through condensation of amino acids are referred to as peptides. Short polymer chains with less than 25 amino acids are called oligopeptides or just

peptides, whereas longer chains are called polypeptides. Proteins are polypeptides formed through ribosomal translations. Primary structure of peptides is the linear sequence of amino acids. Secondary structure is what describes the local conformation of the backbone. Most common conformations are α-helix and β-sheet (Figure 2.6), as well as turns and loops that include β-hairpins, β-spirals and polyproline helices (Dooling and Tirrell 2013).

Self-assembled peptides have been considered as promising biomaterials due to their ease of synthesis through solid-phase methodology, and tunable properties which may provide formation of self-assembled supramolecular structures and incorporation of biological cues, Self-assembly of peptides can be mediated by either weak specific interactions (i.e. hydrogen bonds or π- π stacking) or strong non-specific interactions (i.e. electrostatic), and can be observed in α-helices, β-sheets, coiled-coils or various other naturally occurring motifs (Rivas et al. 2019). EAK16 peptide with a sequence of AEAKAEAKAEAKAEAK was reported to be the first example of peptides that form self-standing gel structure in aqueous solution. Inspired from this sequence Chen and his colleagues prepared three different peptides, EAK16-I,-II and -IV, AEAKAEAKAEAKAEAK (EAK16-I, - + - + - + - +), AEAEAKAKAEAEAKAK (EAK16-II, - - + + - - + +), and AEAEAEAEAKAKAKAK (EAK16-IV, - - - - + + + +), which have the same composition but different sequences to elucidate the effect of charge distribution on self-assembly of designed peptides by using both theoretical and experimental approaches. Their results showed that EAK16-IV formed globular structures with some β-turn content whereas EAK16-I and -II had more extended conformation resulted in fibrillar aggregates (Jun et al. 2004). In another study, they indicated that self-assembled EAK16-IV structures were more susceptible towards the effect of pH, whereas those of EAK16-II showed no significant changes. Between pH values 6.5 and 7.5, EAK16-IV formed globular assemblies and when pH was below 6.5 or above 7.5, these structures transformed into fibrils. However, fibrillar EAK16-II morphology exhibited no drastic changes between pH 4 and 11 (Hong et al. 2003).

Schneider et al. (2002) prepared responsive hydrogels formed via intramolecular folding and self-assembly of a designed peptide, with a sequence of VKVKVKVKVdPPTKVKVKVKV-NH2 denoted as MAX1. By taking advantage of the intramolecular folding propensity of a class of peptides known as β-hairpins, and incorporating ionizable lysine residues into the β-hairpin motif, they managed to tune

gelation of these peptides according to the changes in pH or salt concentration, which led to initial pathway towards the preparation 'smart' materials from β-hairpin family.

2.5.1. Design

Peptides offer a near-infinite design space which can be altered and modified substantially, depending on the desired requirements of the resultant hydrogel. The triggering mechanism for the self-assembly can emerge in various forms, such as pH, heat, salt and light, depending on the judicious choice of the amino acids (Rughani et al. 2010).

Dong et al. (2007) prepared several multidomain peptides having an ABA block motif, with the central B block consisting alternating hydrophilic and hydrophobic amino acids (glutamine and leucine, respectively) and A blocks containing varying number of positively charged lysine residues. The alternating QL pattern allowed the separation of glutamine side chains on one face of the peptide and leucine side chains on the other, creating a facial amphiphile. An aqueous environment would provide a significant driving force for these hydrophobic faces to pack against one another, forming a hydrophobic sandwich that would preserve the extended conformation and stabilize fully. The first group of the synthesized peptides was $K_2(QL)_mK_2$ family, with m values between 2 and 6. Of these peptides $K_2(QL)_6K_2$ was reported to adopt a very strong β-sheet conformation. Then, they tested $K_n(QL)_6K_n$ family of peptides to determine the optimum number of lysine to induce gelation by varying the number of lysines between 1 and 4. Single lysine in A blocks rendered the peptide completely insoluble in aqueous solutions whereas incorporation of three and four K residues disrupted and completed completely eliminated self-assembled fibrous structures, respectively. Addition of negatively charged phosphate multivalent ions in aqueous peptide solutions resulted in the formation of clear, self-supporting gels due to the physically crosslinking of lysine end blocks. More importantly, gelation of these kind of peptides in phosphate buffer saline at physiological conditions indicated that these hydrogels could have a value in cell growth and entrapment applications.

In another study, Aulisa et al. (2009) investigated the effect of sequence on viscoelastic properties of the hydrogels based on another ABA multiblock peptide, by

using negatively charged glutamic acids (E) in the A block and serines (S) as the hydrophilic amino acid in the amphiphilic B block. Changing the composition of A block from lysine (K) to glutamic acid (E) changed the charge of the peptides from positive to negative, allowing them to form gels in the presence of Mg^{2+z}. which can be commonly found in cell culture medium, Using serine instead of glutamine, on the other hand, significantly improved the mechanical properties of the resultant hydrogels, by doubling the storage modules of hydrogels of positively charged peptides in PBS, and increasing that of the negatively charged peptides almost up to 5 times in the presence of Mg^{2+}. Additionally, serine containing hydrogels showed the ability to recover up to 80% of their strength within 1 minute after undergoing shear thinning, whereas glutamine containing peptides were only able to recover up to 50% of their original storage modulus.

Ozbas et al. (2004) studied the effect of salt concentration on the self-assembly, conformation and mechanical properties of hydrogels based on β-hairpin motif, MAX1, which had a random coil conformation at pH 7.4 and low ionic strength. The addition of salt into the solution, however, resulted in the formation of self-assembled structures, rich in β-sheet. MAX1 had a net positive charge at pH 7.4, yet with the addition of Cl^- ions, intramolecular folding event was favored due to the screening of repulsions between the positively charged lysine residues. Rheological experiments proved that the storage moduli of the hydrogels and the kinetics of the self-assembly can be controlled by the ionic strength of the peptide solutions.

Haines et al. (2005) prepared a peptide, MAX7CNB. which formed stable hydrogel after irradiation. Indeed, MAX7CNB was an iteration of the MAX1 peptide. To prepare the light activated β-hairpin peptide, MAX1 was first iterated into MAX7, by replacing valine residue located as 16th amino acid with a cysteine. Required photocage for the peptide was selected as α-carboxy-2-nitrobenzyl due to the negative charge at neutral basic pH, which prevented gelation and the formation of noncytotoxic byproduct after photolysis. Final peptide, MAX7CNB was synthesized by reacting MAX7 with 2-bromo-2-(2-nitrophenyl)acetic acid via a modified protocol originally reported by Bayley and co-workers. Irradiating the solution ($260< \lambda <360$ nm) resulted in the release of the photocage, initiating self-assembly and formation of the hydrogel.

Rajagopal et al. (2009) proposed a pH-dependent strategy to control the thermally triggered folding, self-assembly and hydrogelation of the amphiphilic β-hairpin peptides. Lysine residue were replaced with glutamic acids, threonine or valine systematically to alter the net charge of the self-assembling peptide, MAX1. It was shown that lower net

positive charge resulted in hydrogelation at lower pH values at a given temperature. However, gelation was not only dependent on the net charge but also the location of the substituent within the peptide sequence. Finally, they replaced lysine at position 15 with glutamic acid in MAX1 peptide to prepare MAX1(15E) peptide, which could undergo thermally triggered hydrogelation at physiological conditions (pH 7.4, 150 mM NaCl, 37^{o}C).

2.5.2. Applications

Self-assembling peptides have been proposed in tissue engineering and regeneration applications. (Koutsopoulos 2016). For example, several designed peptides and peptide composites have promoted the growth of pre-osteoblast (Horii et al. 2007) and osteoblast cells (Bokhari et al. 2005). Peptide based hydrogels and scaffolds were also reported to improve cartilage regeneration (Florine et al. 2013), ligament regeneration (Chen et al. 2012), neural tissue formation (Holmes et al. 2000), optical nerve regeneration (Ellis-Behnke et al. 2006), angiogenesis (Wang, Horii, et al. 2008), heart regeneration (Davis et al. 2005), liver regeneration (Wang, Nagrath, et al. 2008), tooth regeneration (Dissanayaka et al. 2015), cochlea cell culture for hearing organ regeneration (Spencer et al. 2008), middle-ear mucosal regeneration (Akiyama et al. 2013) and wound healing processes. (Schneider et al. 2008),

Hydrogels can also be used in drug delivery applications due to their high water content and porosity, both of which are crucial to control diffusion of nutrients, drugs and waste. Fabrication of a drug delivery vehicle can be something as simple as physical entrapment of the drug or something complex, such as immobilization of the drug with covalent bonds. Covalent immobilization can be accomplished by conjugating the drug to the reactive functional groups of a peptide, or an incorporation of the bioactive peptide into the main sequence of a carrier molecule such as polymer if the peptide, itself, is therapeutic. Release of the physically entrapped drugs can be controlled simply by adjusting the mesh size of the hydrogel whereas release of immobilized drugs requires the degradation or disintegration of the whole network. Matrices based on peptide hydrogels were used to encapsulate stem cell secretomes (Bakota et al. 2011), control the release of the neurotrophic growth factors (Lindsey et al. 2015), small molecule drugs

(Li et al. 2016), shear sensitive payloads (Worthington, Langhans, et al. 2017), macromolecules (Branco et al. 2009). Peptide hydrogels were also employed as scaffolds for high-throughput drug screening (Worthington, Drake, et al. 2017). Additionally, if pinpoint accuracy is required in the release of payloads, injectable peptide hydrogels were proposed (Romano et al. 2011).

CHAPTER 3

MATERIALS and METHODS

This chapter consists of the materials and methods applied in this study. Methods include optimization of peptide synthesis protocol, primary characterization of peptides, and preparation and characterization of peptide hydrogels sections.

3.1. Materials

Low loading rink amide MBHA resin, fmoc-protected leucine (L), aspartic acid (D), glutamic acid (E) were purchased from Novabiochem. Fmoc-Protected valine (V) and lysine (K), and coupling agents 1 - [Bis(dimethylamino) methylene] - 1H - 1,2,3 – triazolo [4,5-b]pyridinium 3 – oxidhexafluorophosphate (HATU), O - (1H – 6 – chlorobenzotriazole – 1 – yl) - 1,1,3,3 - tetramethyluronium hexafluorophosphate (HCTU), and N,N-diisopropiletilamin (DIEA) and anisol used in the cleavage and deprotection cocktail were obtained from Carl Roth (Karlsruhe, Germany). Piperidine was (Acros Organics; Geel, Belgium) was used as a deprotecting agent during the peptide synthesis. Dimethylformamide (DMF), trifluoroacetic acid (TFA), l-glutamine, monosodium phosphate (Na_2HPO_4), monopotassium phosphate (KH_2PO_4), sodium chloride (NaCl) were purchased from Merck (Darmstadt, Germany). Hydrochloric acid (HCl) and potassium chloride (KCl) were obtained from Panreac Quimica (Barcelona, Spain) was used to adjust pH. 2-(1H-benzotriazol-1-yl)-1,1,3,3-tetramethyluronium hexafluorophosphate (HBTU), dimethyl sulfoxide (DMSO), dichloromethane (DCM), diethyl ether (DEE), 1,2-ethanedithiol (EDT), thioanisole, sinapic acid, potassium bromide-FTIR grade (KBr), sodium hydroxide (NaOH), acetonitrile, cell counting kit-8 (CCK-8), were purchased from Sigma-Aldrich (St. Louis, MO, USA). Trypsin EDTA Solution C, Dulbecco's modified eagle medium (DMEM) fetal bovine serum (FBS), and gentamycin sulfate (Biological Industries, Cromwell, CT, USA) were used in cell culture experiments. All the reagents were used without purification. Deionized water was used in preparation of aqueous solutions unless specified otherwise.

3.2. Solid Phase Peptide Synthesis

Typical peptide synthesis includes deprotection, activation, coupling, final deprotection steps as shown in Figure 3.1. When the synthesis is completed, peptide is cleaved from the resin and deprotected using an appropriate cocktail depending on the nature of the amino acids in the peptide. In this study, Aapptec Focus Xi (Louisville, KY, USA) automated peptide synthesizer was used to perform the synthesis of the peptides, at a 0.1-mmol scale. In order to optimize the peptide synthesis 3 different methods were applied by changing synthesis solvent and coupling agents, as given in Table 3.1.

Table 3.1. Solvents and coupling agents used in peptide synthesis optimization

Method	Solvent	Coupling Agent
I	DMF	HBTU
II	DMF:DMSO (1:1)	HBTU
III	DMF:DMSO (1:1)	HATU+HCTU

In a typical synthesis, 0.1 mmol resin (0.286g) was placed inside a reaction vessel, and swelled with 4 mL solvent for 10 min, followed by 45 min. Deprotection reactions were carried out by using 20% piperidine solution for 10 min and repeated 3 times. Coupling reactions were performed using 0.4 mmol f-moc protected amino acid and 0.395 mmol coupling agents. Prior to coupling reactions, f-moc protected amino acids were dissolved in 4 ml solvent and then 1 ml DIEA (1 M) was added. The solution was transferred into the reaction vessel to initiate the coupling reaction. Double coupling was used for the entire sequence, with 60 min reaction time per coupling. In method III, for the first five amino acid couplings, HCTU and HATU were used for the first and second couplings, respectively. For the rest of the sequence, HATU was used for both couplings. After the final deprotection step, the resin was washed with copious amount of DCM and dried in vacuum oven in room temperature for 1 h. Then the resin was cleaved and side chains were protected by using Reagent R (TFA:thioanisole:ethanedithiol:anisole = 90:5:3:2) for 2.5 h at room temperature. Next, the resin was separated, and the filtrate was precipitated over cold diethyl ether and centrifuged. The precipitate was washed with diethyl ether and centrifuged twice. Deprotected peptide was dissolved in 10 ml DI water, frozen and freeze-dried. The crude peptide was stored at -20^{o}C. In this study, the peptides, with the sequences and molar masses given in Table 3.2, were synthesized.

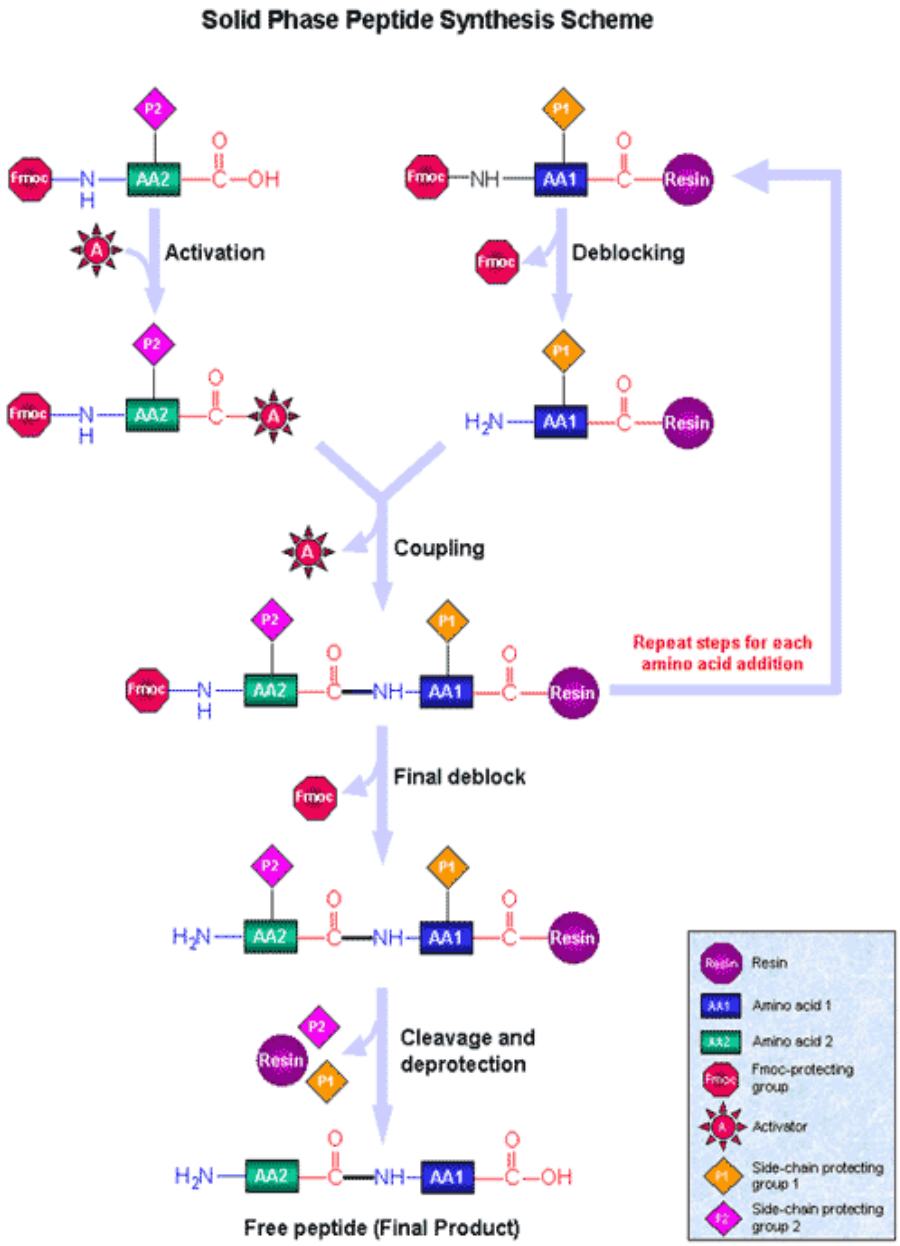

Figure 3.1. Solid Phase Peptide Synthesis (Source: Sigma Aldrich Life Science 2016)

Table 3.2. Sequences and molar masses of the peptides synthesized in this study

Notation	Structure	Molar Mass (Da)
KLEL	KLELKLELKLEL	1467.84
KLDV	KLDVKLDVKLDV	1383.68
KLKV1	KLDVKLDVKLKV	1396.76
KLKV2	KLKVKLDVKLKV	1409.85
KLKV3	KLKVKLKVKLKV	1422.93

3.3. Primary Characterization of Peptides

Purity of the peptides were assessed by using Reverse phase high pressure liquid chromatography (RP-HPLC) and matrix-assisted laser desorption/ionization time of flight mass spectroscopy (MALDI-TOF-MS). RP-HPLC experiments were carried out by using Agilent 1100 Series HPLC (Santa Clara, CA, USA). 0.1% TFA in DI water and 0.08% TFA in Acetonitrile were used as Solvent A and Solvent B, respectively. ~1 mg sample was dissolved in 1 ml of solvent A, filtered, and 100 µl of the sample solution was injected into the C18 or C4 analytical column (Inertsil WP-300, 5 µm, 4.6x100 mm). The column was equilibrated by passing solvent A and solvent B at a ratio of 95:5, then solvent A to solvent B ratio was varied from 95:5 to 30:70, linearly in 65 min. Eluent flow rate was used as 1ml/min and elution profile of the sample was monitored using a UV detector at 214 nm.

Molar masses of the samples were determined by using Bruker Daltonics – Autoflex III Smartbeam model MALDI-TOF-MS, located at Biological Mass Spectrometry and Proteomics Facility located at the Chemistry Department of İzmir Institute of Technology. Prior to the analysis, solution of peptides in 0.1% TFA in deionized water was mixed with sinapic acid, which was used as matrix.

Fourier Transform Infrared Spectroscopy (FTIR) characterization of the samples was carried out on a Shimadzu 8400S model (Tokyo, Japan) spectrophotometer by employing the standard KBr pellet technique. The spectra were taken between 400 cm^{-1} and 4000 cm^{-1} wavenumber range with a scan number of 32 and resolution of 2 cm^{-1}.

3.4. Preparation of Peptide Hydrogels

Gelation of the peptides was performed in deionized water or in PBS buffer at pH 7.4 (137 mM NaCl, 2.7 mM KCl, 8 mM Na_2HPO_4, and 2 mM KH_2PO_4). The peptide was dissolved in DI water at 1 wt% concentration (i.e. 10 mg peptide in 1 ml DI water) and the pH of the solution was gradually increased to 7.4 by using 0.2 M or 1 M NaOH solution. To induce gelation in PBS, peptide was first dissolved in deionized water at 1.5 wt% concentration (890 µl), and then phosphate solution (100 × phosphate, 10 µl) was added, mixed briefly, followed by adding salt solution (10 × salt, 100 µl).

3.5. Characterization of Peptide Hydrogels

Atomic Force Microscopy (AFM) images of the peptide hydrogels, prepared in Milli-Q grade water at 1 wt% concentration was taken using a Digital Instruments-MMSPM Nanoscope lV model instrument. 1 µl of the gel pipetted onto freshly cleaved mica and diluted with 100 µl Milli-Q grade water and then left to dry at room temperature. AFM imaging was performed at room temperature, using tapping mode with a Bruker silicon cantilever tip that has a string constant of 0.4 N/m (Camarillo, CA, USA). The AFM data were analyzed using NanoScope Analysis software (Bruker, US).

Oscillatory rheology experiments of the hydrogels were carried out on a Thermo Fisher Scientific HAAKE MARS Rheometer (Waltham, MA, USA) instrument equipped with a stainless steel parallel plate with a diameter of 35 mm. 1 mL of gel samples, prepared at 1 wt% concentration in DI water or 1.5 wt% in PBS (pH adjusted to 7.4) were placed on the lower plate, and the gap adjusted to 500 µm. Strain sweep experiments were carried out at 1 Hz and frequency sweep tests were performed at a constant strain of 0.02% within a frequency range of 0.1 to 100 Hz.

Cell proliferation studies were done by using L929 mouse fibroblast cell line based on sets of three independent hydrogel samples and control samples. The cells were cultivated in DMEM cell medium containing 2 mM glutamine, 10% fetal bovine serum (FBS) and 50 µg/ml gentamycin sulfate. Peptides were first treated with HCl to replace TFA salts. For this procedure, peptides were dissolved at 1 mg/ml DI water concentration, and then 100 mM HCl was added to reach a final concentration of 5 mM HCl, followed by freezing the solution and subsequently, lyophilization. This process was repeated 3 times. 1.5 wt% concentration peptide HCl salt solution was prepared in PBS buffer at pH 7.4, according to the procedure given in section 3.4. Prior to gelation 100 µl of the peptide solution was placed in the each corresponding well of the 96-well microplate and then allowed to gel for 1 h. Empty tissue culture treated polystyrene (TCPS) was used as the control group. 100 µl L929 cell solution (2.5×10^4 cell/ml in cultivation medium) was added to each well and the microplates were incubated at 37 °C in 5% CO_2 atmosphere for 1 and 3 days. To determine cell proliferation, 10 µl CCK-8 solution was added to each well and the microplates were incubated for 2 h. Absorbance values at 450 nm ($A_{450\ nm}$) were measured using Thermo Fisher Varioskan Flash microplate reader (Waltham, MA, USA).

CHAPTER 4

RESULTS and DISCUSSION

In the first part of this chapter, an optimal peptide synthesis procedure giving the highest peptide purity was selected out of the three methods. Then purity assessment and conformation results of the peptides, along with the preparation and characterization results of peptide hydrogels are given.

4.1. Optimization of Peptide Synthesis Protocol

Three different peptide synthesis methods, as outlined in Table 3.1, were compared according to the purity of the resultant KLEL peptide. In order to assess the purity of the peptide, RP-HPLC and MALDI-TOF-MS analyses were used. HPLC traces and MALDI-TOF mass spectra of KLEL peptides, synthesized according to Method I, Method II and Method III are given in Figure 4.1, Figure 4.2 and Figure 4.3 respectively.

In all of the MALDI-TOF mass spectra of the peptides, $(M+H^+)$, (M+Na) and (M+K) adduct peaks were observed but with a +3 Da difference from the theoretical value, which can be related to the calibration of the instrument. KLEL peptide synthesized according to Method II and Method III looked almost pure, as indicated by a few small impurity peaks in mass spectra as shown in Figure 4.2a and Figure 4.3a, respectively. Higher number of impurity peaks, on the other hand, were observed in mass spectrum of KLEL peptide, synthesized according to Method I. Comparison of mass spectra of the peptides suggested that the use of mixed DMSO-DMF solvents in the peptide synthesis provided higher purity of the resultant peptide independent of the nature of the coupling agent.

HPLC chromatograms of KLEL peptide, synthesized according to Method I and Method II, were obtained by using C18 column, and showed a broad peak, composed of a few to several resolved sharp peaks, between 40 min and 60 min. The use of C4 column in the HPLC analysis, on the other hand, gave a better resolution of the peaks in this region, as given in Figure 4.2c and Figure 4.3b. Thus, as observed for other hydrophobic

peptides, strong interaction of the peptide with the column caused the broadening of the peaks and complicated the assessment of the purity of the peptides (Hood et al. 2008). Nevertheless, appropriate synthesis protocols were selected according to the mass spectroscopy results.

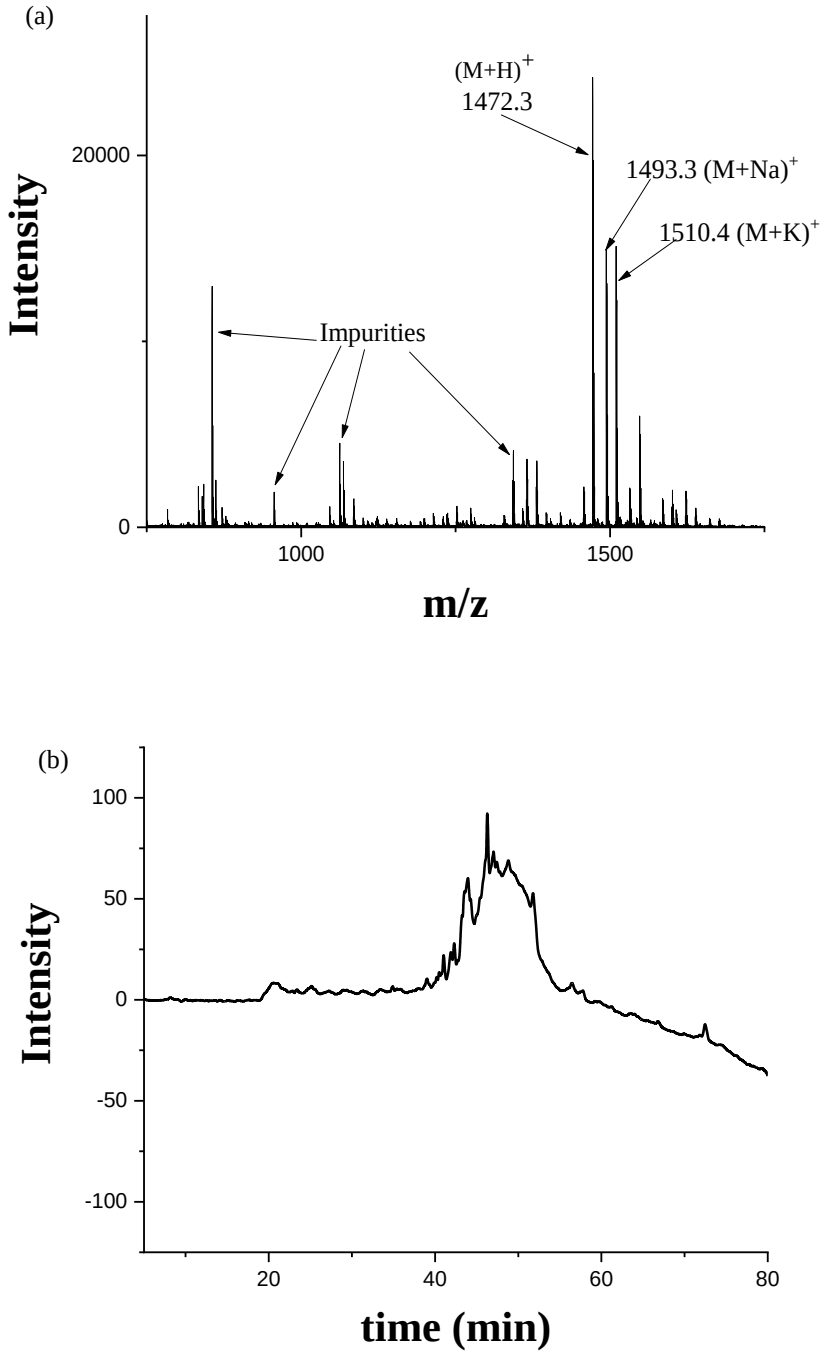

Figure 4.1. (a) MALDI-TOF-Mass spectrum, (b) HPLC traces obtained by using C18 column of KLEL peptide synthesized according to Method I

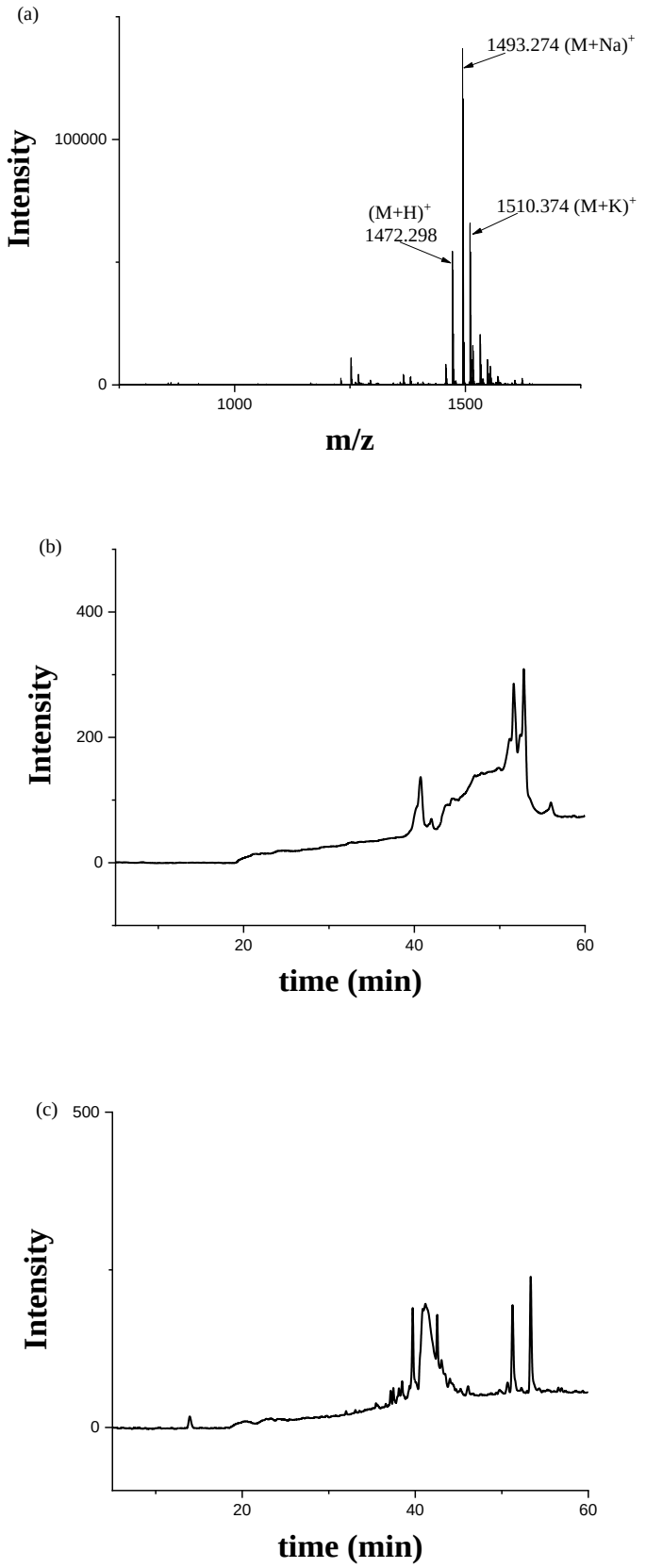

Figure 4.2. (a) MALDI-TOF-Mass spectrum, (b) HPLC traces obtained by using C18, (c) C4 column of KLEL peptide synthesized according to Method II

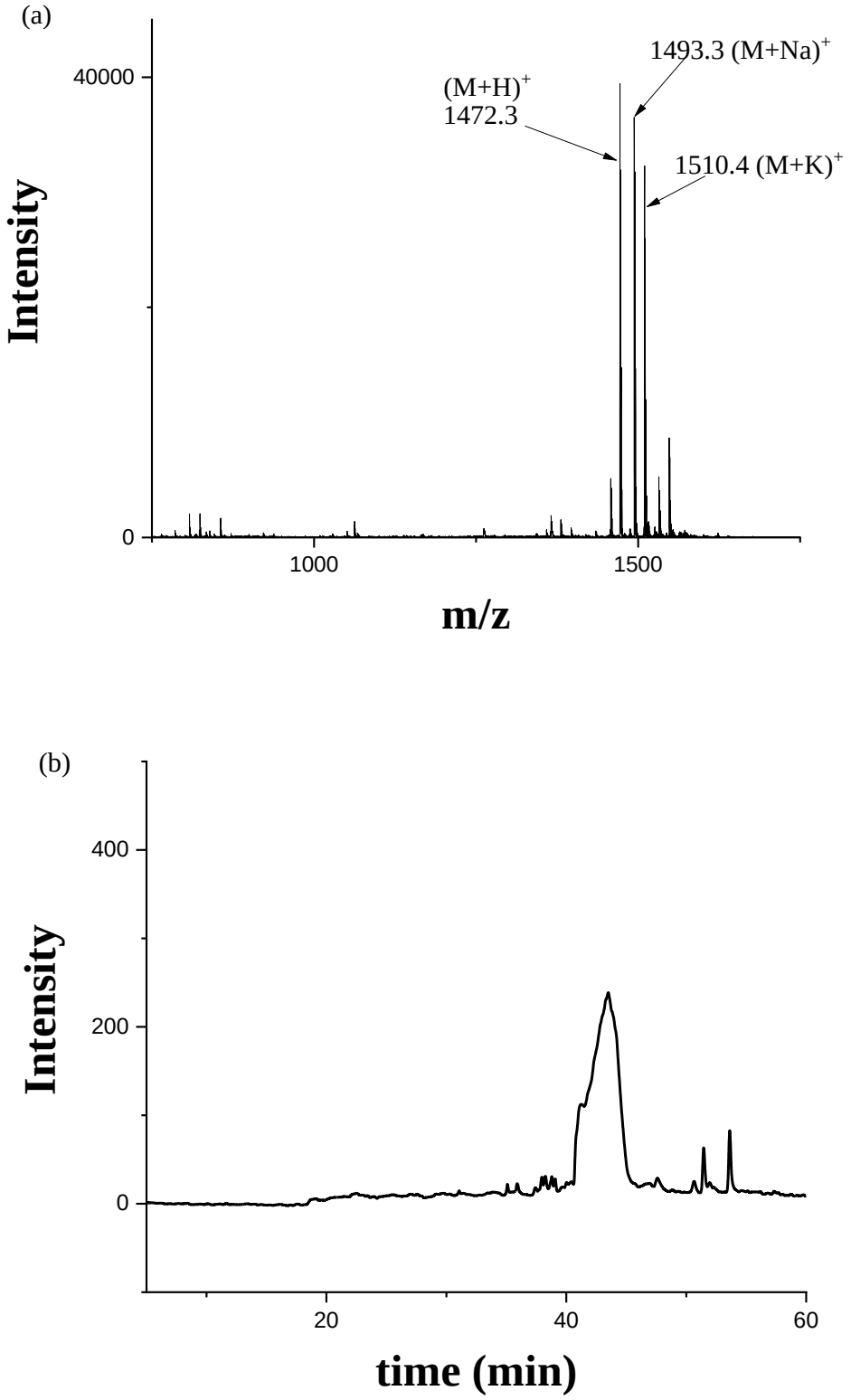

Figure 4.3. (a) MALDI-TOF-Mass spectrum, (b) HPLC traces obtained by using C18 column of KLEL peptide synthesized according to Method III

4.2. Primary Characterization of Peptides

KLXV family of peptides, where X = D or K, given in Table 3.2, were synthesized according to Method III. MALDI-TOF mass spectra and HPLC chromatograms of KLDV, KLKV1, KLKV2 and KLKV3 peptides were given in Figure 4.4, Figure 4.5, Figure 4.6 and Figure 4.7, respectively. In the mass spectra of all peptides, +3 Da shift was observed in the $(M+H)^+$, (M+Na) and (M+K) adduct peaks. (M+DMSO) adduct was also identified in the KLDV peptide. In addition to these main peaks, a few small impurity peaks were apparent in mass spectra of KLDV and KLKV3, the peptides with regular sequences. However, higher percentage of impurities was suggested by the mass spectra of KLKV1 and KLKV2. Indeed, the presence of adducts obscured the spectra. For this reason, the peptides should be purified preferentially by ziptip, prior to the analyses.

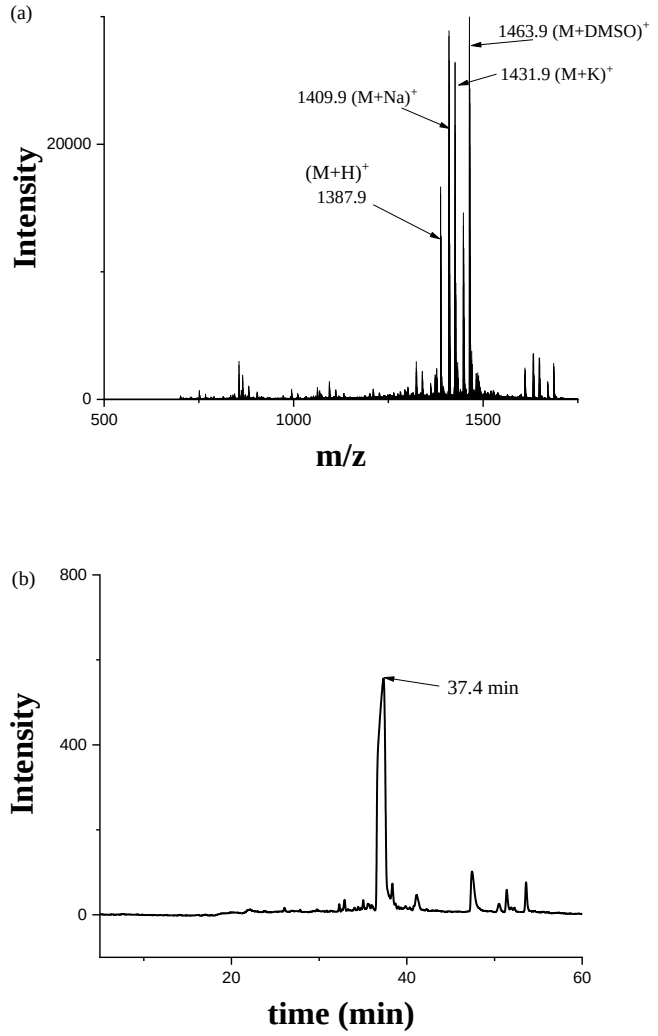

Figure 4.4. (a) MALDI-TOF mass spectrum, (b) HPLC traces of KLDV peptide

KLDV, KLKV1, KLKV2 and KLKV3 eluted at 37.4 min, 34.7 min, 33.2 min and 31.8 min, respectively, with quite narrow peaks compared to that of KLEL peptide. In addition to these main peaks, a few small impurity peaks were also observed in all of the HPLC chromatograms.

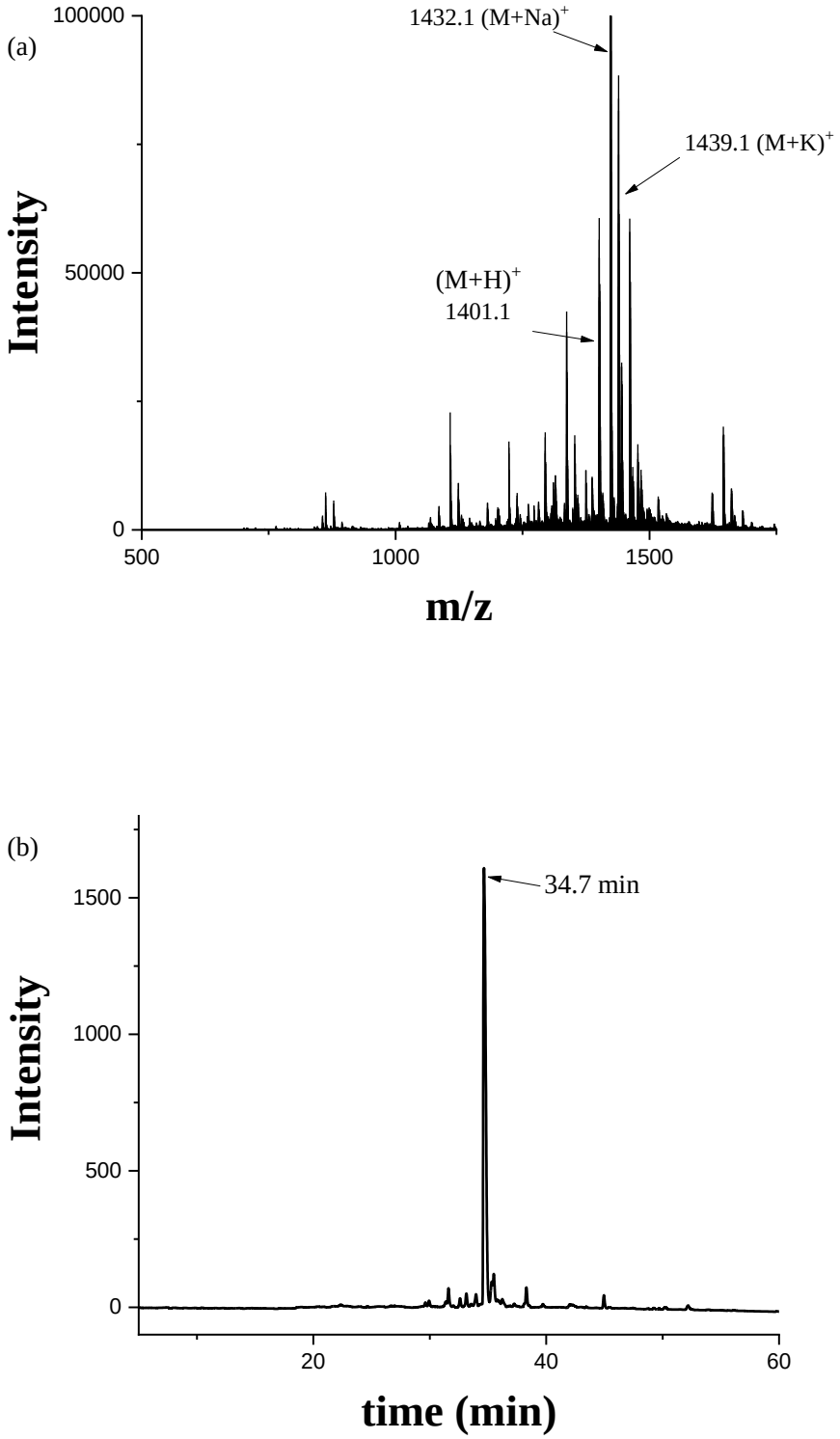

Figure 4.5. (a) MALDI-TOF mass spectrum, (b) HPLC traces of KLKV1 peptide

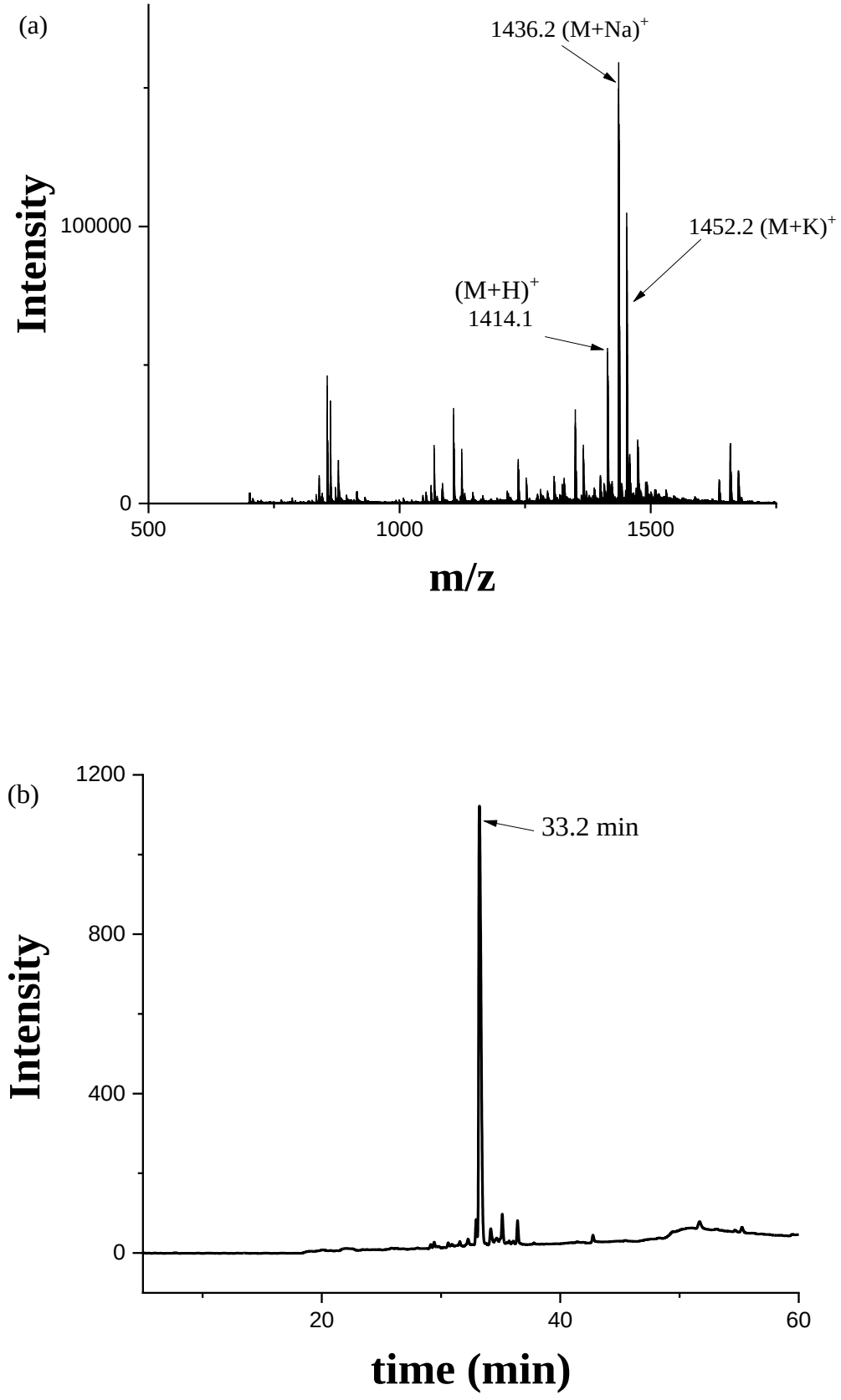

Figure 4.6. (a) MALDI-TOF mass spectrum, (b) HPLC traces of KLKV2 peptide

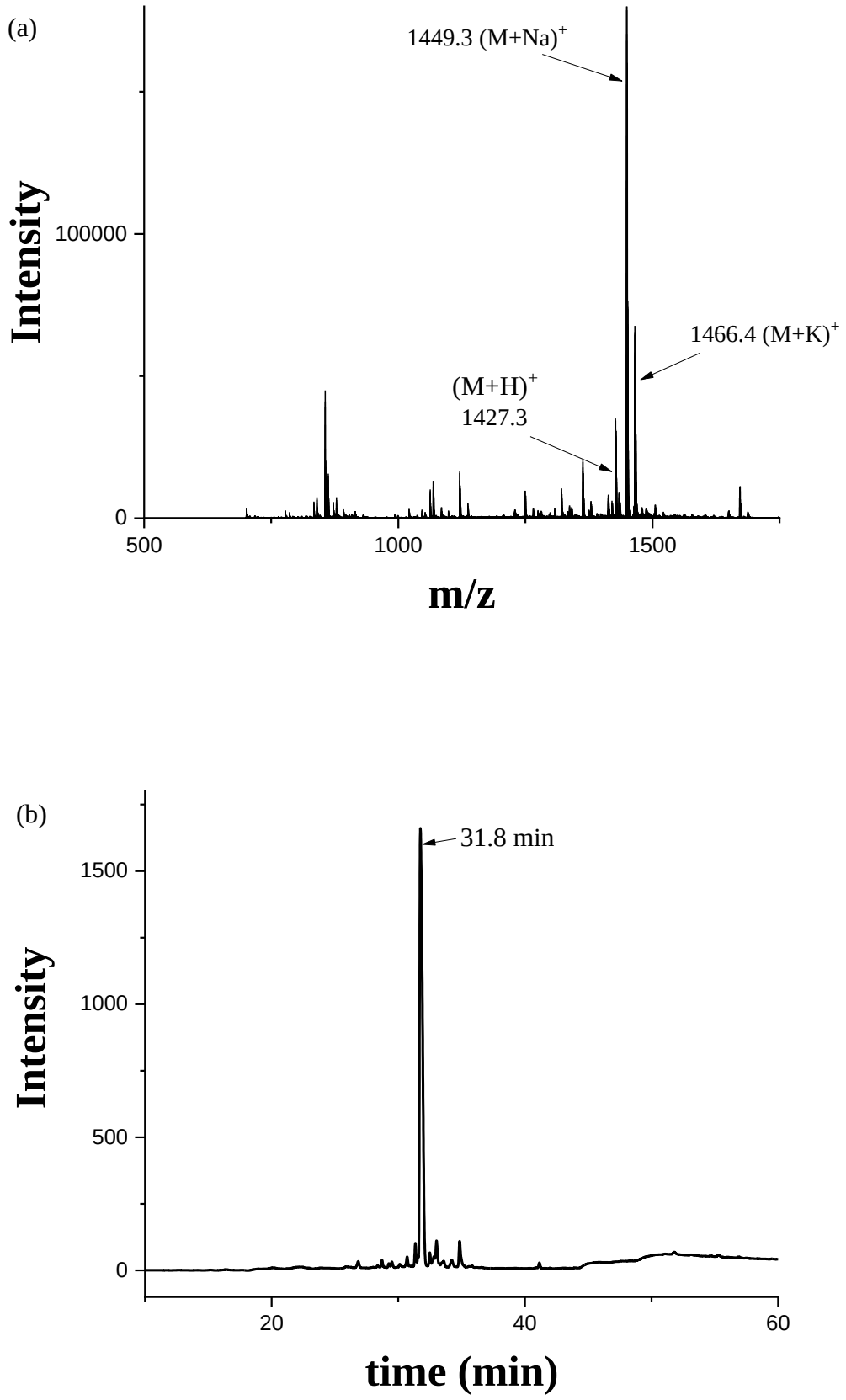

Figure 4.7. (a) MALDI-TOF mass spectrum, (b) HPLC traces of KLKV3 peptide

FTIR spectra of KLXV family of peptides are given in Figure 4.8. In all spectra, characteristic infrared bands of peptide linkage, Amide I (1600-1690 cm^{-1}, C=O stretching), Amide II (1480-1575 cm^{-1}, CN stretching, NH bending), Amide III (1229-1301 cm^{-1}, CN stretching, NH bending), Amide A (3300 cm^{-1}, NH Stretching) and Amide B (3100 cm^{-1}, NH stretching) bands were observed, as expected (Kong and Yu 2007). Amide I region of the spectra is given in Figure 4.9. In this region, a sharp peak around 1630 cm^{-1}, which indicated that the peptides were rich in β-sheet secondary structure was obtained. In addition to this, ta broad peak between 1650-1700 cm^{-1} was also apparent, associated with TFA interference, which overshadowed the secondary structure information in this region (Lembre et al. 2014). Thus, HCl salt of peptides should be prepared and used in FTIR analyses.

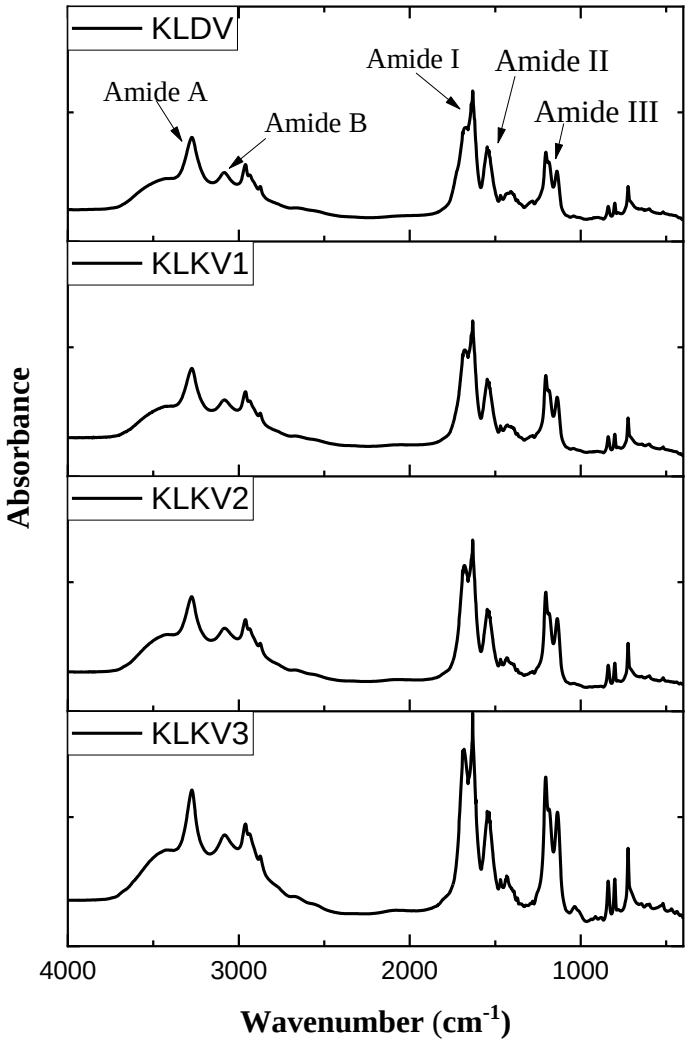

Figure 4.8. FTIR spectra of KLXV family of peptides

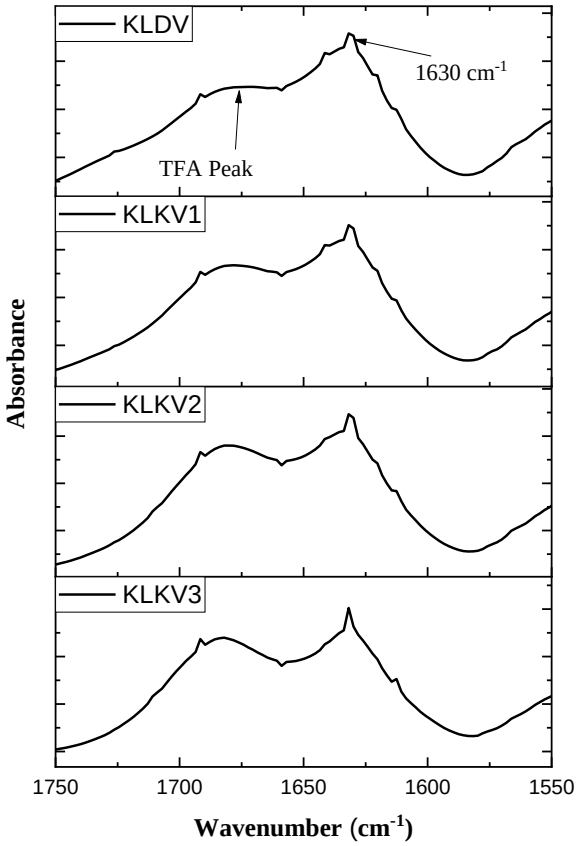

Figure 4.9. Amide I FTIR spectra of KLXV family of peptides.

4.3. Preparation of Hydrogels

KLXV family of peptides formed hydrogels in DI water at 1 wt% concentration upon increasing the pH to neutral pH, indicating the pH responsiveness of these peptides. Self-standing peptide hydrogels obtained in DI water are given in Figure 4.10.

Figure 4.10. KLXV family of peptide hydrogels prepared in DI water

Dissolution of peptides directly in 1 × PBS buffer at pH 7.4 was resulted in the precipitation of the peptides and in some cases, microgels. Therefore, hydrogels were prepared according to the method described in section 3.4, in which 100 × phosphate and 10 × salt, were used. Only KLDV and KLKV1 out of four KLXV family of peptides formed hydrogels by applying this method, but at 1.5 wt% concentration. Pictures of the hydrogels prepared in PBS buffer are given in Figure 4.11.

Figure 4.11. KLDV and KLKV1 hydrogels prepared in PBS

4.4. Characterization of Peptide Hydrogels

Morphology of KLXV peptide hydrogels were determined by using AFM technique. AFM images of the hydrogels, based on KLDV, KLKV1, KLKV2 and KLKV3 peptides are given in Figure 4.12, Figure 4.13, Figure 4.14 and Figure 4.15, respectively.

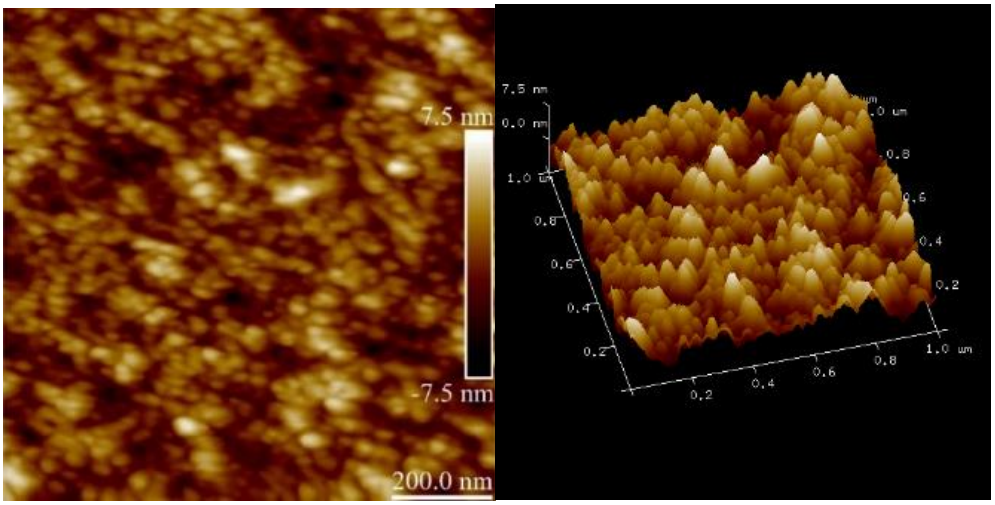

Figure 4.12. 2D and 3D AFM images of KLDV hydrogel

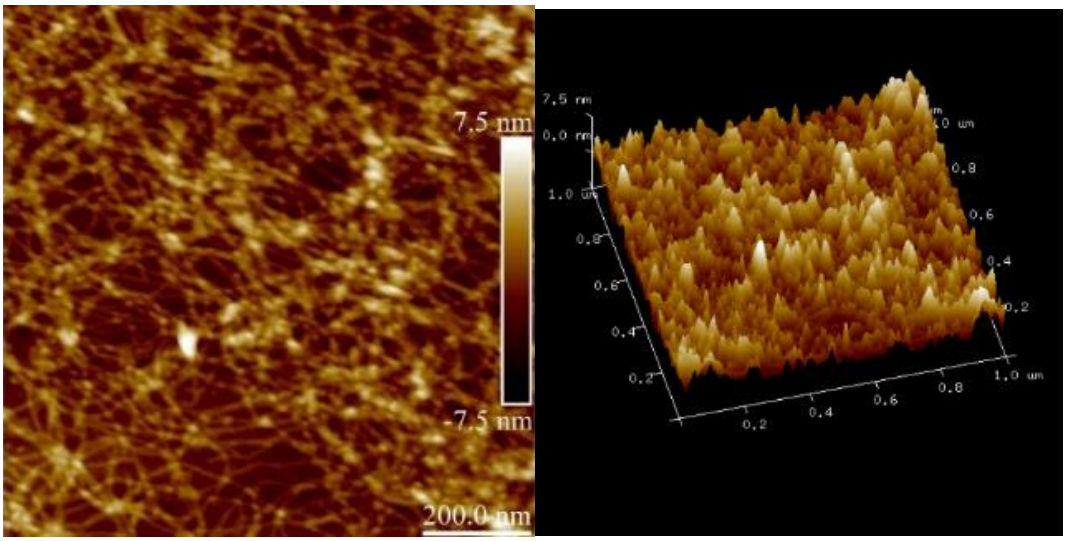

Figure 4.13. 2D and 3D AFM images of KLKV1 hydrogel

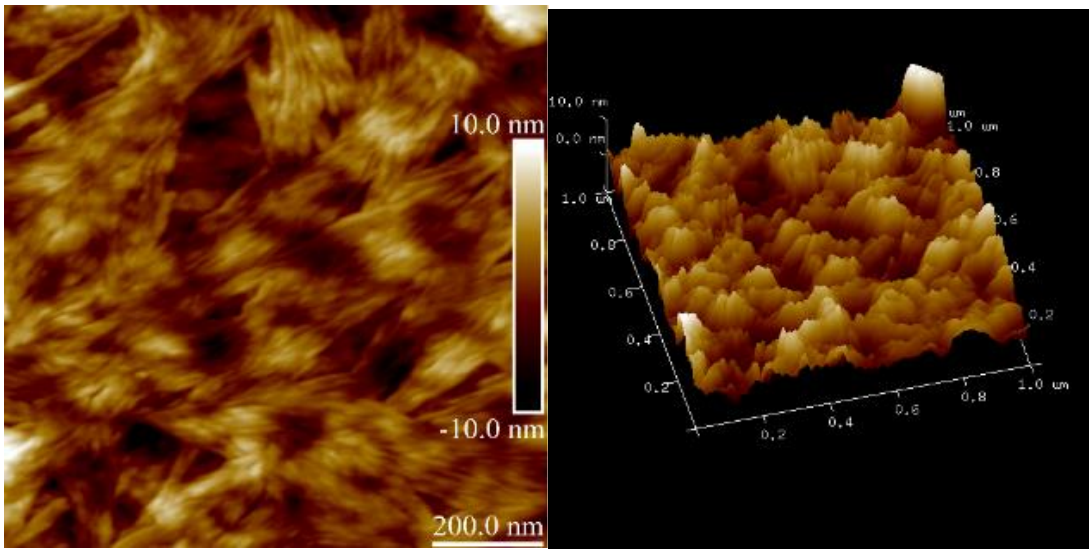

Figure 4.14. 2D and 3D AFM images of KLKV2 hydrogel

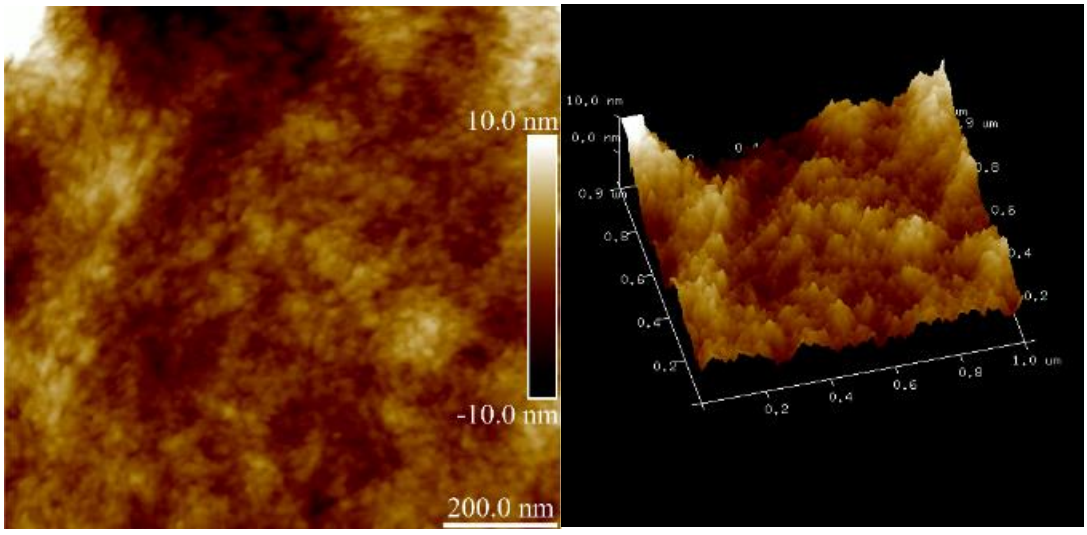

Figure 4.15. 2D and 3D AFM images of KLKV3 hydrogel

In the AFM images, globular, fibrous and a mixture of globular and fibrous structures were observed, depending on the peptide sequence. In general, peptides with regular sequences tend to form globular structures. Mean sizes of these globular structures were obtained as ~30 nm and ~10 nm for KLDV and KLKV3, respectively. KLKV2, on the other hand, presented non-uniform stacked fibrillar structures, with individual fibril widths ranging between 7-18 nm. Stacking of the fibrils could be resulted from drying of the hydrogels during the sample preparation. KLKV1 exhibited a distinct network structure, composed of both fibrous and globular structures with sizes ranging between 5-20 nm. Fibrillar, rather than globular structures, have been most commonly observed for peptide hydrogels. For example RADA16 (Cormier et al. 2013), RATEA16 (Zhao et al. 2008) and MASP1 (Lin et al. 2014) peptides were reported to form fibrillar structures with sizes in the order of 3 to 10 nm.

Viscoelastic properties of peptide hydrogels were determined by using oscillatory rheometer measurements. Strain sweep and frequency sweep data are given in Figures from 4.16 to 4.19 for KLVX family of peptide hydrogels prepared in DI water. Figure 4.20 and Figure 4.21 represent strain sweep and frequency sweep data for KLDV and KLKV1 hydrogel prepared in PBS, respectively. Strain sweep experiments were carried out to determine the linear viscoelastic region of the hydrogels. For hydrogels prepared in DI water, the linear region was observed between 0.01% and 0.07% whereas for hydrogels prepared in PBS, it was observed to range between 0.01% and 0.05%. Therefore 0.02% strain was selected to be used in frequency sweep experiments. In all frequency sweep data, G' (storage modulus) was obtained higher than G" (loss modulus), confirming the gel structure. G' values of the hydrogels, that corresponds to the plateau region of frequency sweep data are summarized and compared with those of multidomain peptide hydrogels prepared by Hartgerink group in Table 4.1. G' values of KLXV family of peptide hydrogels prepared in DI water ranged between ~200 Pa and ~2000 Pa. The most striking result was that hydrogels based on regular peptides (KLDV and KLKV3), exhibited a much higher mechanical strength, despite their unconventional morphology. G' values of KLDV and KLKV1 peptide hydrogels were observed to be higher in PBS compared to those obtained in DI water, which could be attributed to higher concentration of the gels prepared in PBS buffer. For multidomain peptides, addition of cell attachment unit (GRGDS group) into the β-sheet forming unit tend to decrease storage moduli of the resultant hydrogel. On the other hand, incorporation of LDV sequence into the β-sheet forming unit, as in this study, can impart cell attachment ability to hydrogels without

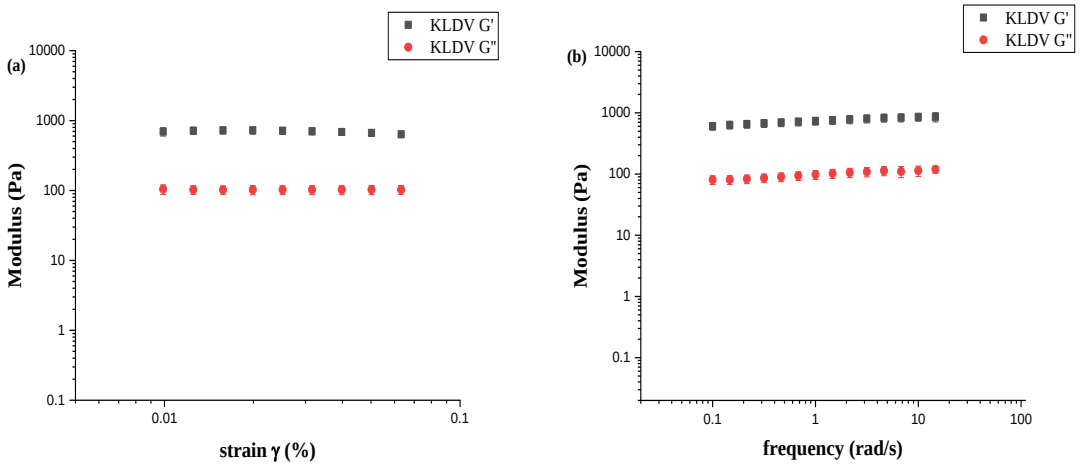

Figure 4.16. (a) Strain sweep and (b) frequency sweep data for KLDV hydrogel in DI water

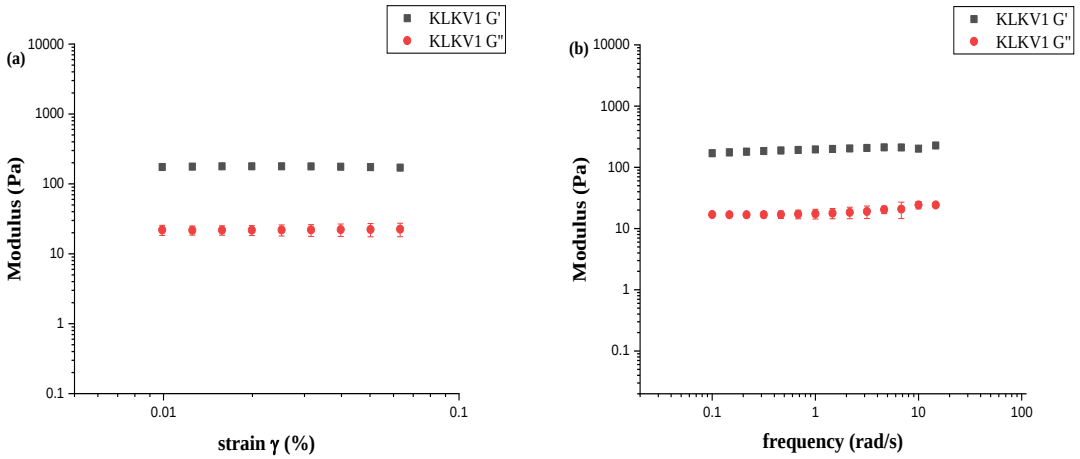

Figure 4.17. (a) Strain sweep and (b) frequency sweep data for KLKV1 hydrogel in DI water

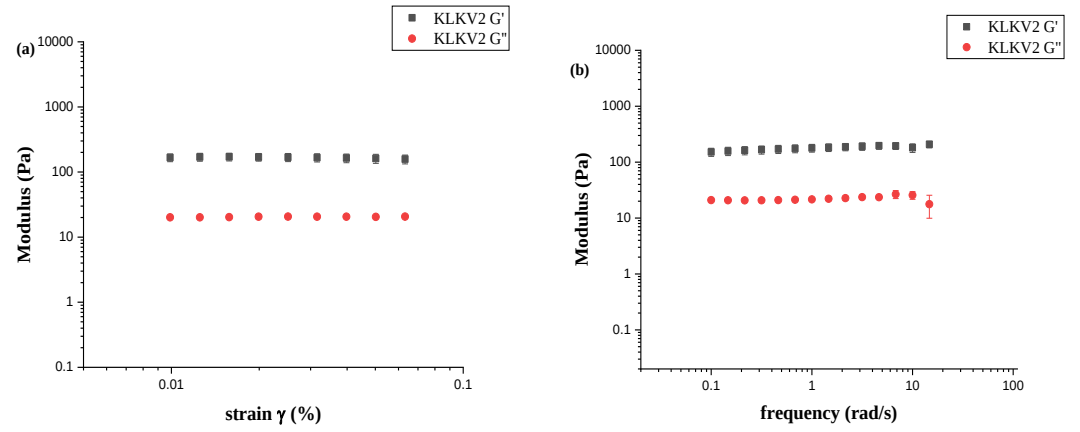

Figure 4.18. (a) Strain sweep and (b) frequency sweep data for KLKV2 hydrogel in DI water

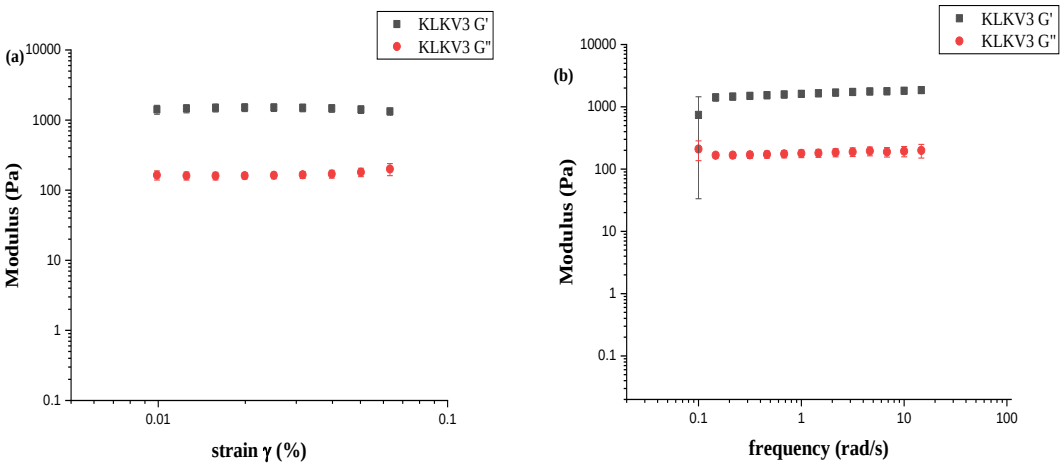

Figure 4.19. (a) Strain sweep and (b) frequency sweep data for KLKV3 hydrogel in DI water

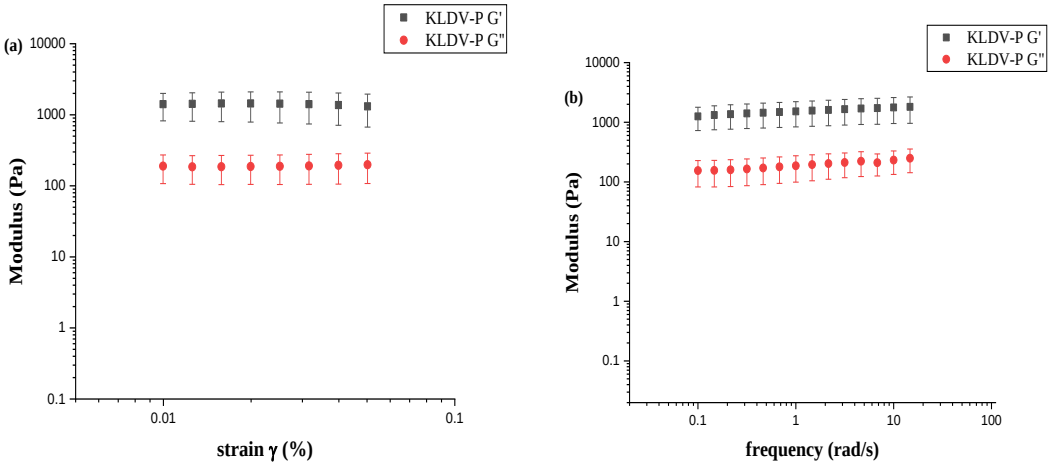

Figure 4.20. (a) Strain sweep and (b) frequency sweep data for KLDV hydrogel in PBS

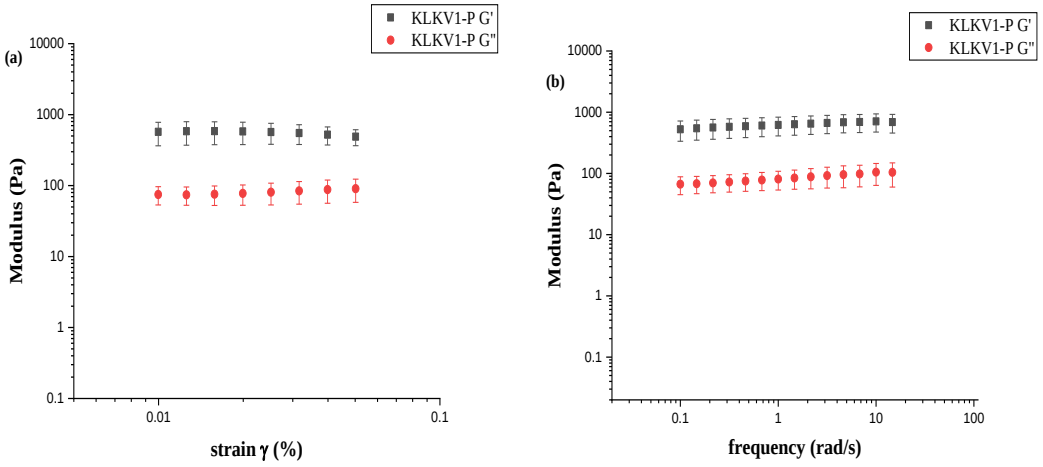

Figure 4.21. (a) Strain sweep and (b) frequency sweep data for KLKV1 hydrogel in PBS

Table 4.1. Comparison of the G' values of KLXV hydrogels and MDP hydrogels

Peptide	Structure	Solvent	Storage Modulus (Pa)	Reference
MDP1	$K_2(SL)_6K_2$	PBS	~400	(Galler et al. 2010)
MDP2	$K_2(SL)_6K_2$GRGDS		~160	
MDP3	$K_2(SL)_3RG(SL)_3K_2$		~50	
MDP4	$K(SL)_3RG(SL)_3K$		~190	
MDP5	$K(SL)_3RG(SL)_3K$GRGDS		~180	
KLDV	$(KLDV)_3$	DIW	860±150	This Study
KLKV1	$(KLDV)_2KLKV$		263±56	
KLKV2	$KLDV(KLKV)_2$		210±30	
KLKV3	$(KLKV)_3$		1850±200	
KLDV	$(KLDV)_3$	PBS	1810±850	
KLKV1	$(KLDV)_2KLKV$		700±230	

sacrificing the mechanical strength of the hydrogels. Nevertheless, we observed that a peptide hydrogel with 3 LDV repeats had much higher storage modulus than the one with 2 LDV repeats.

Cell proliferation tests were done using CCK-8 assay. Prior to the experiments HCl salt form of KLDV and KLKV1 were prepared to avoid the toxic effect of TFA, associated with crude peptide, by applying the procedure outlined in section 3.5. Absorbance values measured at 450 nm, which correlates the number of cells, obtained for the peptide hydrogels and the TCPS wells at the end of day 1 and day 3, are given in Figure 4.22. It was observed that both hydrogels promoted cell proliferation slightly better than empty TCPS wells at the end of the first day. Although the number of cells increased as expected, no significant difference in cell proliferation was observed after 3 days for all samples. Similar cell proliferation promoting abilities of the peptide hydrogels and empty TCPS well are quite promising as most of the hydrogels despite their RGD content exhibited inferior performance compared to TCPS alone (Bradshaw et al. 2014, Shu et al. 2004b)

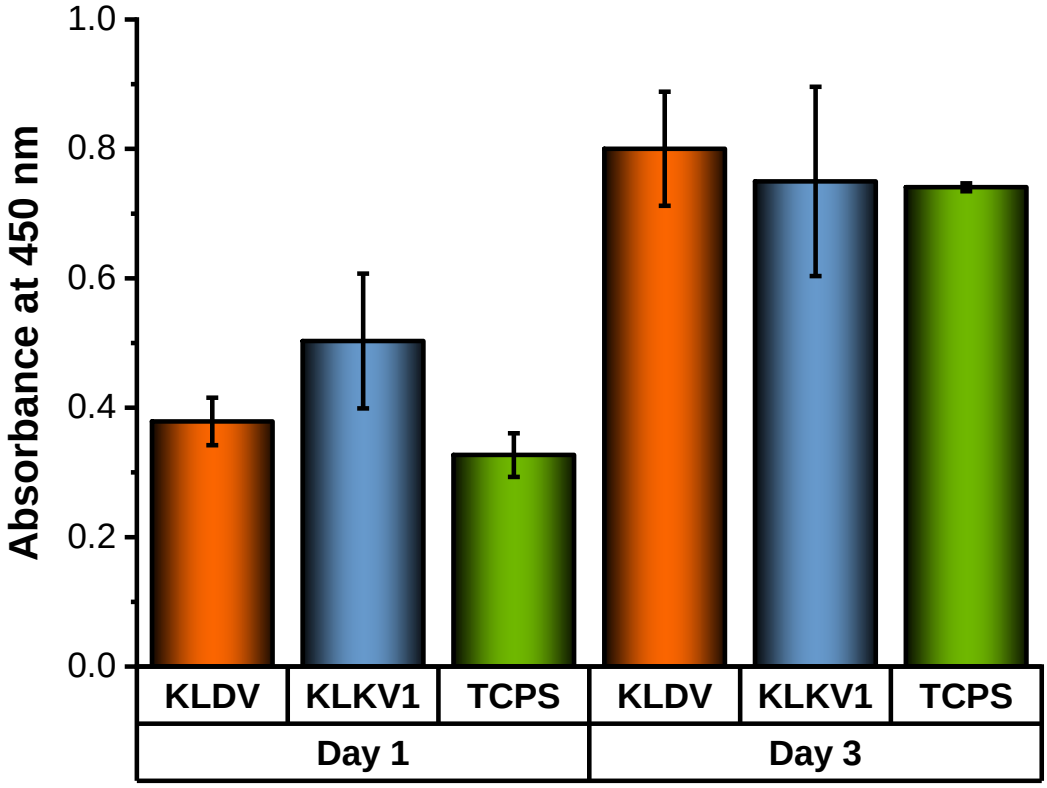

Figure 4.22. Cell Proliferation data of KLDV, KLKV1 hydrogels and empty TCPS well obtained at the end of 1st and 3rd day.

CHAPTER 5

CONCLUSIONS and FUTURE WORK

In this study, a number of β-sheet forming peptides were synthesized by employing f-moc strategy in SPPS. For some peptides, LDV sequence was incorporated into the β -sheet forming domain with the intention of increasing cell proliferation and attachment. Prior to the synthesis of KLXV family peptides, peptide synthesis procedure was optimized by employing three different methods in the synthesis of KLEL peptide synthesis. According to the MALDI-TOF-MS results, the use of DMF-DMSO (1:1) solvent mixture resulted in peptides with higher purity, independent of the nature of the coupling agent. FTIR spectroscopy of the peptides confirmed β-sheet secondary structure, however, between 1650-1700 cm^{-1} region of the spectra was obscured by TFA, preventing the determination of other secondary structures, thus FTIR experiments will be carried out by using the HCl salt form of the peptides. Additionally, Circular Dichroic (CD) spectroscopy should be used to determine the secondary structure in low concentration region. All the peptides formed self-standing hydrogels in DI water at 1 wt% concentration after reaching neutral pH. AFM results of the hydrogels indicated that peptides with regular repeats unexpectedly formed globular structures whereas the rest formed fibrous structures. As a complementary study, TEM will also be used to determine the morphology of the hydrogels. It was also observed that these regular peptides exhibited higher mechanical strength. Only HCl salt form of peptides with higher LDV content were able to form hydrogels in PBS but requiring 1.5 wt% concentration. Hydrogels prepared in PBS were also stronger, which can be attributed to their higher peptide wt% concentration. CCK-8 assay results indicated that these hydrogels promoted cell growth as much as TCPS, which suggests the use of these peptide hydrogels in soft tissue engineering applications, however, cell adhesion and migration tests should be performed in order to elucidate the effect of LDV sequence.

Future studies will include gelation in cell culture medium and tests of these hydrogels 3D cell culture systems.

REFERENCES

Abd Alla, Safaa G., Murat Sen, and Abdel Wahab M. El-Naggar. 2012. "Swelling and mechanical properties of superabsorbent hydrogels based on Tara gum/acrylic acid synthesized by gamma radiation." *Carbohydrate Polymers* 89 (2):478-485. doi: https://doi.org/10.1016/j.carbpol.2012.03.031.

Akiyama, N., T. Yamamoto-Fukuda, H. Takahashi, and T. Koji. 2013. "In situ tissue engineering with synthetic self-assembling peptide nanofiber scaffolds, PuraMatrix, for mucosal regeneration in the rat middle-ear." *Int J Nanomedicine* 8:2629-40. doi: 10.2147/IJN.S47279.

Andreopoulos, F. M., E. J. Beckman, and A. J. Russell. 1998. "Light-induced tailoring of PEG-hydrogel properties." *Biomaterials* 19 (15):1343-52.

Aulisa, L., H. Dong, and J. D. Hartgerink. 2009. "Self-assembly of multidomain peptides: sequence variation allows control over cross-linking and viscoelasticity." *Biomacromolecules* 10 (9):2694-8. doi: 10.1021/bm900634x.

Bakota, E. L., Y. Wang, F. R. Danesh, and J. D. Hartgerink. 2011. "Injectable multidomain peptide nanofiber hydrogel as a delivery agent for stem cell secretome." *Biomacromolecules* 12 (5):1651-7. doi: 10.1021/bm200035r.

Bokhari, M. A., G. Akay, S. Zhang, and M. A. Birch. 2005. "The enhancement of osteoblast growth and differentiation in vitro on a peptide hydrogel-polyHIPE polymer hybrid material." *Biomaterials* 26 (25):5198-208. doi: 10.1016/j.biomaterials.2005.01.040.

Bradshaw, M., D. Ho, M. W. Fear, F. Gelain, F. M. Wood, and K. S. Iyer. 2014. "Designer self-assembling hydrogel scaffolds can impact skin cell proliferation and migration." *Sci Rep* 4:6903. doi: 10.1038/srep06903.

Branco, M. C., D. J. Pochan, N. J. Wagner, and J. P. Schneider. 2009. "Macromolecular diffusion and release from self-assembled beta-hairpin peptide hydrogels." *Biomaterials* 30 (7):1339-47. doi: 10.1016/j.biomaterials.2008.11.019.

Brondsted, H, L Hovgaard, and L Simonsen. 1995. "Dextran hydrogels for colon-specific drug-delivery. 4. Comparative release study of hydrocortisone and prednisolone sodium-phosphate." *STP Pharma Sciences* 5 (1):65-69.

Cappello, J, JW Crissman, M Crissman, FA Ferrari, G Textor, O Wallis, JR Whitledge, Xia Zhou, D Burman, and L Aukerman. 1998. "In-situ self-assembling protein polymer gel systems for administration, delivery, and release of drugs." *Journal of Controlled Release* 53 (1-3):105-117.

Cappello, Joseph, John Crissman, Mary Dorman, Marcia Mikolajczak, Garret Textor, Magda Marquet, and Franco Ferrari. 1990. "Genetic engineering of structural protein polymers." *Biotechnology progress* 6 (3):198-202.

Chen, K., S. Sahoo, P. He, K. S. Ng, S. L. Toh, and J. C. Goh. 2012. "A hybrid silk/RADA-based fibrous scaffold with triple hierarchy for ligament regeneration." *Tissue Eng Part A* 18 (13-14):1399-409. doi: 10.1089/ten.TEA.2011.0376.

Chirani, Naziha, Lukas Gritsch, Federico Leonardo Motta, and Silvia Fare. 2015. "History and applications of hydrogels." *Journal of biomedical sciences* 4 (2).

Chung, Hyun Jung, and Tae Gwan Park. 2009. "Self-assembled and nanostructured hydrogels for drug delivery and tissue engineering." *Nano Today* 4 (5):429-437. doi: 10.1016/j.nantod.2009.08.008.

Cormier, Ashley R, Xiaodong Pang, Maxwell I Zimmerman, Huan-Xiang Zhou, and Anant K Paravastu. 2013. "Molecular structure of RADA16-I designer self-assembling peptide nanofibers." *ACS nano* 7 (9):7562-7572.

Coviello, Tommasina, Mario Grassi, Giuseppe Rambone, Eleonora Santucci, Maria Carafa, Evelina Murtas, Fulvio M. Riccieri, and Franco Alhaique. 1999. "Novel

hydrogel system from scleroglucan: synthesis and characterization." *Journal of Controlled Release* 60 (2):367-378. doi: https://doi.org/10.1016/S0168-3659(99)00091-7.

Davis, M. E., J. P. Motion, D. A. Narmoneva, T. Takahashi, D. Hakuno, R. D. Kamm, S. Zhang, and R. T. Lee. 2005. "Injectable self-assembling peptide nanofibers create intramyocardial microenvironments for endothelial cells." *Circulation* 111 (4):442-50. doi: 10.1161/01.CIR.0000153847.47301.80.

Dissanayaka, W. L., K. M. Hargreaves, L. Jin, L. P. Samaranayake, and C. Zhang. 2015. "The interplay of dental pulp stem cells and endothelial cells in an injectable peptide hydrogel on angiogenesis and pulp regeneration in vivo." *Tissue Eng Part A* 21 (3-4):550-63. doi: 10.1089/ten.TEA.2014.0154.

Dong, He, Sergey E. Paramonov, Lorenzo Aulisa, Erica L. Bakota, and Jeffrey D. Hartgerink. 2007. "Self-Assembly of Multidomain Peptides: Balancing Molecular Frustration Controls Conformation and Nanostructure." *Journal of the American Chemical Society* 129 (41):12468-12472. doi: 10.1021/ja072536r.

Dooling, Lawrence J., and David A. Tirrell. 2013. "Peptide and Protein Hydrogels." In *Polymeric and Self Assembled Hydrogels: From Fundamental Understanding to Applications*, 93-124. The Royal Society of Chemistry.

Eagland, D, NJ Crowther, and CJ Butler. 1994. "Complexation between polyoxyethylene and polymethacrylic acid—the importance of the molar mass of polyoxyethylene." *European polymer journal* 30 (7):767-773.

Ellis-Behnke, Rutledge G., Yu-Xiang Liang, Si-Wei You, David K. C. Tay, Shuguang Zhang, Kwok-Fai So, and Gerald E. Schneider. 2006. "Nano neuro knitting: Peptide nanofiber scaffold for brain repair and axon regeneration with functional return of vision." *Proceedings of the National Academy of Sciences of the United States of America* 103 (13):5054-5059. doi: 10.1073/pnas.0600559103.

Florine, E. M., R. E. Miller, R. M. Porter, C. H. Evans, B. Kurz, and A. J. Grodzinsky. 2013. "Effects of Dexamethasone on Mesenchymal Stromal Cell

Chondrogenesis and Aggrecanase Activity: Comparison of Agarose and Self-Assembling Peptide Scaffolds." *Cartilage* 4 (1):63-74. doi: 10.1177/1947603512455196.

Gacesa, Peter. 1988. "Alginates." *Carbohydrate polymers* 8 (3):161-182.

Galler, Kerstin M, Lorenzo Aulisa, Katherine R Regan, Rena N D'Souza, and Jeffrey D Hartgerink. 2010. "Self-assembling multidomain peptide hydrogels: designed susceptibility to enzymatic cleavage allows enhanced cell migration and spreading." *Journal of the American Chemical Society* 132 (9):3217-3223.

Gehrke, Stevin H., Lorelle H. Uhden, and James F. McBride. 1998. "Enhanced loading and activity retention of bioactive proteins in hydrogel delivery systems." *Journal of Controlled Release* 55 (1):21-33. doi: https://doi.org/10.1016/S0168-3659(98)00019-4.

Gombotz, Wayne R, and SiowFong Wee. 1998. "Protein release from alginate matrices." *Advanced drug delivery reviews* 31 (3):267-285.

Goosen, Mattheus FA, Geraldine M O'Shea, Hrire M Gharapetian, Sheng Chou, and Anthony M Sun. 1985. "Optimization of microencapsulation parameters: semipermeable microcapsules as a bioartificial pancreas." *Biotechnology and bioengineering* 27 (2):146-150.

Green, Hodaya, Guy Ochbaum, Anna Gitelman-Povimonsky, Ronit Bitton, and Hanna Rapaport. 2018. "RGD-presenting peptides in amphiphilic and anionic β-sheet hydrogels for improved interactions with cells." *RSC Advances* 8 (18):10072-10080. doi: 10.1039/c7ra12503h.

Haines, Lisa A., Karthikan Rajagopal, Bulent Ozbas, Daphne A. Salick, Darrin J. Pochan, and Joel P. Schneider. 2005. "Light-Activated Hydrogel Formation via the Triggered Folding and Self-Assembly of a Designed Peptide." *Journal of the American Chemical Society* 127 (48):17025-17029. doi: 10.1021/ja054719o.

Holmes, Todd C., Sonsoles de Lacalle, Xing Su, Guosong Liu, Alexander Rich, and Shuguang Zhang. 2000. "Extensive neurite outgrowth and active synapse formation on self-assembling peptide scaffolds." *Proceedings of the National Academy of Sciences* 97 (12):6728-6733. doi: 10.1073/pnas.97.12.6728.

Hong, Yooseong, Raymond L. Legge, S. Zhang, and P. Chen. 2003. "Effect of Amino Acid Sequence and pH on Nanofiber Formation of Self-Assembling Peptides EAK16-II and EAK16-IV." *Biomacromolecules* 4 (5):1433-1442. doi: 10.1021/bm0341374.

Hood, Christina A, German Fuentes, Hirendra Patel, Karen Page, Mahendra Menakuru, and Jae H Park. 2008. "Fast conventional Fmoc solid-phase peptide synthesis with HCTU." *Journal of peptide science: an official publication of the European Peptide Society* 14 (1):97-101.

Horii, A., X. Wang, F. Gelain, and S. Zhang. 2007. "Biological designer self-assembling peptide nanofiber scaffolds significantly enhance osteoblast proliferation, differentiation and 3-D migration." *PLoS One* 2 (2):e190. doi: 10.1371/journal.pone.0000190.

Hubbell, Jeffrey A. 1996. "Hydrogel systems for barriers and local drug delivery in the control of wound healing." *Journal of Controlled Release* 39 (2-3):305-313.

Humphries, J. D., A. Byron, and M. J. Humphries. 2006. "Integrin ligands at a glance." *J Cell Sci* 119 (Pt 19):3901-3. doi: 10.1242/jcs.03098.

Jameela, SR, and A Jayakrishnan. 1995. "Glutaraldehyde cross-linked chitosan microspheres as a long acting biodegradable drug delivery vehicle: studies on the in vitro release of mitoxantrone and in vivo degradation of microspheres in rat muscle." *Biomaterials* 16 (10):769-775.

Jayawarna, Vineetha, Murtza Ali, Thomas A Jowitt, Aline F Miller, Alberto Saiani, Julie E Gough, and Rein V Ulijn. 2006. "Nanostructured hydrogels for three-dimensional cell culture through self-assembly of fluorenylmethoxycarbonyl–dipeptides." *Advanced Materials* 18 (5):611-614.

Jonker, Anika M, Dennis WPM Löwik, and Jan CM van Hest. 2012. "Peptide-and protein-based hydrogels." *Chemistry of Materials* 24 (5):759-773.

Jun, S., Y. Hong, H. Imamura, B. Y. Ha, J. Bechhoefer, and P. Chen. 2004. "Self-assembly of the ionic peptide EAK16: the effect of charge distributions on self-assembly." *Biophys J* 87 (2):1249-59. doi: 10.1529/biophysj.103.038166.

Kang, M. K., J. S. Colombo, R. N. D'Souza, and J. D. Hartgerink. 2014. "Sequence effects of self-assembling multidomain peptide hydrogels on encapsulated SHED cells." *Biomacromolecules* 15 (6):2004-11. doi: 10.1021/bm500075r.

Kong, Jilie, and Shaoning Yu. 2007. "Fourier transform infrared spectroscopic analysis of protein secondary structures." *Acta biochimica et biophysica Sinica* 39 (8):549-559.

Koutsopoulos, S. 2016. "Self-assembling peptide nanofiber hydrogels in tissue engineering and regenerative medicine: Progress, design guidelines, and applications." *J Biomed Mater Res A* 104 (4):1002-16. doi: 10.1002/jbm.a.35638.

Lee, Kuen Yong, and David J Mooney. 2001. "Hydrogels for tissue engineering." *Chemical reviews* 101 (7):1869-1880.

Lembre, P., P. Di Martino, and C. Vendrely. 2014. "Amyloid peptides derived from CsgA and FapC modify the viscoelastic properties of biofilm model matrices." *Biofouling* 30 (4):415-26. doi: 10.1080/08927014.2014.880112.

Li, I. C., A. N. Moore, and J. D. Hartgerink. 2016. ""Missing Tooth" Multidomain Peptide Nanofibers for Delivery of Small Molecule Drugs." *Biomacromolecules* 17 (6):2087-95. doi: 10.1021/acs.biomac.6b00309.

Lin, Yi-An, Yu-Chuan Ou, Andrew G Cheetham, and Honggang Cui. 2014. "Rational design of MMP degradable peptide-based supramolecular filaments." *Biomacromolecules* 15 (4):1419-1427.

Lindsey, S., J. H. Piatt, P. Worthington, C. Sonmez, S. Satheye, J. P. Schneider, D. J. Pochan, and S. A. Langhans. 2015. "Beta Hairpin Peptide Hydrogels as an Injectable Solid Vehicle for Neurotrophic Growth Factor Delivery." *Biomacromolecules* 16 (9):2672-83. doi: 10.1021/acs.biomac.5b00541.

Mahler, Assaf, Meital Reches, Meirav Rechter, Smadar Cohen, and Ehud Gazit. 2006. "Rigid, self-assembled hydrogel composed of a modified aromatic dipeptide." *Advanced Materials* 18 (11):1365-1370.

Mohd Amin, Mohd Cairul Iqbal, Naveed Ahmad, Nadia Halib, and Ishak Ahmad. 2012. "Synthesis and characterization of thermo- and pH-responsive bacterial cellulose/acrylic acid hydrogels for drug delivery." *Carbohydrate Polymers* 88 (2):465-473. doi: https://doi.org/10.1016/j.carbpol.2011.12.022.

Ozbas, Bulent, Juliana Kretsinger, Karthikan Rajagopal, Joel P. Schneider, and Darrin J. Pochan. 2004. "Salt-Triggered Peptide Folding and Consequent Self-Assembly into Hydrogels with Tunable Modulus." *Macromolecules* 37 (19):7331-7337. doi: 10.1021/ma0491762.

Patil, Nitin S., Jonathan S. Dordick, and David G. Rethwisch. 1996. "Macroporous poly(sucrose acrylate) hydrogel for controlled release of macromolecules." *Biomaterials* 17 (24):2343-2350. doi: https://doi.org/10.1016/S0142-9612(96)00089-0.

Patil, Nitin S., Yanzi Li, David G. Rethwisch, and Jonathan S. Dordick. 1997. "Sucrose diacrylate: A unique chemically and biologically degradable crosslinker for polymeric hydrogels." *Journal of Polymer Science Part A: Polymer Chemistry* 35 (11):2221-2229. doi: 10.1002/(sici)1099-0518(199708)35:11<2221::Aid-pola12>3.0.Co;2-g.

Rajagopal, K., M. S. Lamm, L. A. Haines-Butterick, D. J. Pochan, and J. P. Schneider. 2009. "Tuning the pH responsiveness of beta-hairpin peptide folding, self-assembly, and hydrogel material formation." *Biomacromolecules* 10 (9):2619-25. doi: 10.1021/bm900544e.

Rashid, Mahmood A, Firas Khatib, and Abdul Sattar. 2015. "Protein preliminaries and structure prediction fundamentals for computer scientists." *arXiv preprint arXiv:1510.02775*.

Rivas, M., L. J. Del Valle, C. Aleman, and J. Puiggali. 2019. "Peptide Self-Assembly into Hydrogels for Biomedical Applications Related to Hydroxyapatite." *Gels* 5 (1). doi: 10.3390/gels5010014.

Romano, N. H., D. Sengupta, C. Chung, and S. C. Heilshorn. 2011. "Protein-engineered biomaterials: nanoscale mimics of the extracellular matrix." *Biochim Biophys Acta* 1810 (3):339-49. doi: 10.1016/j.bbagen.2010.07.005.

Rughani, Ronak V., Monica C. Branco, Darrin J. Pochan, and Joel P. Schneider. 2010. "De Novo Design of a Shear-Thin Recoverable Peptide-Based Hydrogel Capable of Intrafibrillar Photopolymerization." *Macromolecules* 43 (19):7924-7930. doi: 10.1021/ma1014808.

Schneider, A., J. A. Garlick, and C. Egles. 2008. "Self-assembling peptide nanofiber scaffolds accelerate wound healing." *PLoS One* 3 (1):e1410. doi: 10.1371/journal.pone.0001410.

Schneider, Joel P, Darrin J Pochan, Bulent Ozbas, Karthikan Rajagopal, Lisa Pakstis, and Juliana Kretsinger. 2002. "Responsive hydrogels from the intramolecular folding and self-assembly of a designed peptide." *Journal of the American Chemical Society* 124 (50):15030-15037.

Schnepp, Zoe AC, Rosanna Gonzalez-McQuire, and Stephen Mann. 2006. "Hybrid Biocomposites Based on Calcium Phosphate Mineralization of Self-Assembled Supramolecular Hydrogels." *Advanced Materials* 18 (14):1869-1872.

Shu, X. Z., K. Ghosh, Y. Liu, F. S. Palumbo, Y. Luo, R. A. Clark, and G. D. Prestwich. 2004a. "Attachment and spreading of fibroblasts on an RGD peptide-modified injectable hyaluronan hydrogel." *J Biomed Mater Res A* 68 (2):365-75. doi: 10.1002/jbm.a.20002.

Shu, Xiao Zheng, Kaustabh Ghosh, Yanchun Liu, Fabio S Palumbo, Yi Luo, Richard A Clark, and Glenn D Prestwich. 2004b. "Attachment and spreading of fibroblasts on an RGD peptide–modified injectable hyaluronan hydrogel." *Journal of Biomedical Materials Research Part A: An Official Journal of The Society for Biomaterials, The Japanese Society for Biomaterials, and The Australian Society for Biomaterials and the Korean Society for Biomaterials* 68 (2):365-375.

Sigma Aldrich Life Science. 2016. "Solid Phase Synthesis." accessed 22 May 2016. https://www.sigmaaldrich.com/life-science/custom-oligos/custom-peptides/learning-center/solid-phase-synthesis.html.

Spencer, N. J., D. A. Cotanche, and C. M. Klapperich. 2008. "Peptide- and collagen-based hydrogel substrates for in vitro culture of chick cochleae." *Biomaterials* 29 (8):1028-42. doi: 10.1016/j.biomaterials.2007.11.006.

Sperinde, Jeffrey J., and Linda G. Griffith. 1997. "Synthesis and Characterization of Enzymatically-Cross-Linked Poly(ethylene glycol) Hydrogels." *Macromolecules* 30 (18):5255-5264. doi: 10.1021/ma970345a.

Ullah, F., M. B. Othman, F. Javed, Z. Ahmad, and H. Md Akil. 2015. "Classification, processing and application of hydrogels: A review." *Mater Sci Eng C Mater Biol Appl* 57:414-33. doi: 10.1016/j.msec.2015.07.053.

Veiga, A. S., C. Sinthuvanich, D. Gaspar, H. G. Franquelim, M. A. Castanho, and J. P. Schneider. 2012. "Arginine-rich self-assembling peptides as potent antibacterial gels." *Biomaterials* 33 (35):8907-16. doi: 10.1016/j.biomaterials.2012.08.046.

Wang, S., D. Nagrath, P. C. Chen, F. Berthiaume, and M. L. Yarmush. 2008. "Three-dimensional primary hepatocyte culture in synthetic self-assembling peptide hydrogel." *Tissue Eng Part A* 14 (2):227-36. doi: 10.1089/tea.2007.0143.

Wang, Xiumei, Akihiro Horii, and Shuguang Zhang. 2008. "Designer functionalized self-assembling peptide nanofiber scaffolds for growth, migration, and

tubulogenesis of human umbilical vein endothelial cells." *Soft Matter* 4 (12). doi: 10.1039/b807155a.

Willmott, N, HMH Kamel, J Cummings, JFB Stuart, and AT Florence. 1984. "Adriamycin-loaded albumin microspheres: lung entrapment and fate in the rat." In *Microspheres and Drug Therapy*, 205-216. Elsevier Amsterdam.

Worthington, P., K. M. Drake, Z. Li, A. D. Napper, D. J. Pochan, and S. A. Langhans. 2017. "Beta-hairpin hydrogels as scaffolds for high-throughput drug discovery in three-dimensional cell culture." *Anal Biochem* 535:25-34. doi: 10.1016/j.ab.2017.07.024.

Worthington, P., S. Langhans, and D. Pochan. 2017. "Beta-hairpin peptide hydrogels for package delivery." *Adv Drug Deliv Rev* 110-111:127-136. doi: 10.1016/j.addr.2017.02.002.

Yamada, K. M. 1991. "Adhesive recognition sequences." *J Biol Chem* 266 (20):12809-12.

Yamamoto, Masaya, Yasuhiko Tabata, Liu Hong, Susumu Miyamoto, Nobuo Hashimoto, and Yoshito Ikada. 2000. "Bone regeneration by transforming growth factor β1 released from a biodegradable hydrogel." *Journal of Controlled Release* 64 (1-3):133-142.

Yang, F., C. G. Williams, D. A. Wang, H. Lee, P. N. Manson, and J. Elisseeff. 2005. "The effect of incorporating RGD adhesive peptide in polyethylene glycol diacrylate hydrogel on osteogenesis of bone marrow stromal cells." *Biomaterials* 26 (30):5991-8. doi: 10.1016/j.biomaterials.2005.03.018.

Yokoyama, F, I Masada, K Shimamura, T Ikawa, and K Monobe. 1986. "Morphology and structure of highly elastic poly (vinyl alcohol) hydrogel prepared by repeated freezing-and-melting." *Colloid and Polymer Science* 264 (7):595-601.

Zhang, F., G. S. Shi, L. F. Ren, F. Q. Hu, S. L. Li, and Z. J. Xie. 2009. "Designer self-assembling peptide scaffold stimulates pre-osteoblast attachment, spreading and

proliferation." *J Mater Sci Mater Med* 20 (7):1475-81. doi: 10.1007/s10856-009-3700-x.

Zhang, Yan, Zhimou Yang, Fang Yuan, Hongwei Gu, Ping Gao, and Bing Xu. 2004. "Molecular recognition remolds the self-assembly of hydrogelators and increases the elasticity of the hydrogel by 106-fold." *Journal of the American Chemical Society* 126 (46):15028-15029.

Zhao, Ying, Hidenori Yokoi, Masayoshi Tanaka, Takatoshi Kinoshita, and Tianwei Tan. 2008. "Self-assembled pH-responsive hydrogels composed of the RATEA16 peptide." *Biomacromolecules* 9 (6):1511-1518.